



**Auditory Cues in the Perception of Self-Motion for Linear  
Translation**

**Bill Kapralos**

**Daniel Zikovitz**

**Michael R. M. Jenkin**

**Laurence R. Harris**

Technical Report CS-2004-04

November 15, 2004

Department of Computer Science and Engineering  
4700 Keele Street North York, Ontario M3J 1P3 Canada

# Auditory Cues in the Perception of Self-Motion for Linear Translation<sup>5 6</sup>

*B. Kapralos*<sup>1,4</sup>, *D. Zikovitz*<sup>2,4</sup>, *M. R. Jenkin*<sup>1,4</sup> and *L. R. Harris*<sup>3,4</sup>

<sup>1</sup> Dept. of Computer Science and Engineering, <sup>3</sup> Dept. of Psychology, <sup>4</sup> Centre for Vision Research  
York University, Toronto, Ontario, Canada. M3J 1P3

<sup>2</sup> Defence Research and Development Canada,  
Toronto, Ontario, Canada. M3M 3B9

{billk, jenkin}@cs.yorku.ca   Daniel.Zikovitz@drdc-rddc.gc.ca   harris@yorku.ca

## Abstract

A series of experiments that investigate the relative roles of physical motion and changing sound source intensity cues to the perception of linear self-motion. Self-motion was simulated using either (i) physical motion only, (ii) simulated auditory motion only, (iii) physical motion coupled with auditory motion, or (iv) physically moving audio only. In all conditions an over-estimation of self-motion was observed that varied systematically with the simulated acceleration. Of particular interest was that auditory cues combined with physical motion cues resulted in more accurate estimates of self-motion than did either auditory or physical motion cues in isolation.

---

<sup>5</sup>The help by Konstantinos Derpanis is gratefully acknowledged. Konstantinos helped in construction of the apparatus, provided ideas and insight throughout the entire process and was the first to experiment with any of our test iterations. The financial support of NSERC, CRESTech and a York University President's Dissertation Scholarship to B. Kapralos is also appreciated.

<sup>6</sup>A condensed version of this report appears in the Proceedings of the 116<sup>th</sup> Convention of the Audio Engineering Society, Berlin, Germany, May 8-11, 2004.

# Contents

<b>1</b>	<b>Introduction</b>	<b>1</b>
1.1	Overview of this report . . . . .	2
<b>2</b>	<b>Background</b>	<b>3</b>
2.1	Auditory motion cues . . . . .	3
2.2	Acoustical time-to-contact . . . . .	7
2.2.1	Intensity based acoustical tau . . . . .	7
2.3	Summary . . . . .	8
<b>3</b>	<b>Experimental Method</b>	<b>10</b>
3.1	Subjects . . . . .	10
3.2	Equipment . . . . .	10
3.2.1	Subject motion cart and assembly . . . . .	10
3.2.2	Loudspeaker motion cart and assembly . . . . .	11
3.2.3	Motor and motor controller . . . . .	11
3.2.4	Auditory stimuli . . . . .	12
3.3	Experimental procedure . . . . .	15
3.3.1	Experiment one: physical motion only . . . . .	17
3.3.2	Experiment two: simulated auditory motion only . . . . .	17
3.3.3	Experiment three: physical motion + auditory motion . . . . .	17
3.3.4	Experiment four: physically moving audio . . . . .	18
<b>4</b>	<b>Results</b>	<b>19</b>
4.1	Experiment one: physical motion only . . . . .	19
4.2	Experiment two: simulated auditory motion only . . . . .	20
4.3	Experiment three: physical motion + auditory motion . . . . .	20
4.4	Experiment four: physically moving audio . . . . .	21
4.5	Effects of condition . . . . .	21
4.6	Effect of acceleration . . . . .	22

<b>5</b>	<b>Discussion</b>	<b>25</b>
5.1	Experiment one: physical motion only . . . . .	25
5.2	Experiment two: simulated auditory motion only . . . . .	26
5.3	Experiment three: physical motion + auditory motion . . . . .	26
5.4	Experiment four: physically moving audio . . . . .	26
<b>6</b>	<b>Conclusions</b>	<b>28</b>
<b>A</b>	<b>Accurate measure of physical motion</b>	<b>30</b>
A.1	Distance recording equipment . . . . .	30
A.1.1	Mouse operation . . . . .	31
A.1.2	Modifying the serial mouse for use in these experiments . . . . .	33
A.1.3	Communicating with the serial mouse . . . . .	37
<b>B</b>	<b>Motor assembly and controller</b>	<b>38</b>
B.1	Motor and motor controller . . . . .	38
B.2	Track . . . . .	39
B.3	Controlling the motor . . . . .	41
B.3.1	Controller programs: source code . . . . .	44



# Chapter 1

## Introduction

We are capable of judging our own self-motion and the motion of objects as we move about our natural three-dimensional environment. This judgment is based on information arising from several sensory modalities, including visual, auditory and vestibular. Although the literature is still lacking with respect to systematic studies of self-motion perception, available studies have focused primarily on visual and vestibular cues. These studies have found we over-estimate our self-motion when using visual or vestibular cues solely or in conjunction, although we are more accurate when both cues are available (see [19, 22, 30]). In other words, the distance we perceive ourselves to have moved is greater than the actual distance moved and the perceived self-motion changes with cues that present. Visual and vestibular cues are not the only self-motion cues available. Auditory cues may also provide motion information and may actually interact with the visual and vestibular cues. Despite the potential importance of dynamic auditory localization where either the sound source or the observer is moving, few studies have examined the effects on audio cues on the perception of self-motion. In addition, the majority of available literature on auditory cues to self-motion focuses primarily on constant velocity motion, ignoring acceleration, the required stimulus for the vestibular system.

Given the importance of auditory motion cues and auditory localization cues in general in the understanding of our natural surroundings, it is important to understand their contribution to self-motion perception. This report describes four experiments that examine our ability to judge the distance of self-motion when either auditory or physical motion cues were presented independently or in conjunction. In each experiment, subjects are presented with a physical target at a pre-defined distance in front of them. After viewing and becoming familiarized with the target and its position, subjects were blindfolded and either i) physically moved (accelerated) towards the target in the presence or absence of a stationary auditory stimulus, ii) remained stationary while the sound level of a stationary sound source was decreased or iii) remained stationary while the sound stimulus was physically moved (accelerated) away them. Subjects indicated when they perceived that they had reached the presented target. Our results are compared to the perception of self-motion determined by visual and vestibular cues [19].

## 1.1 Overview of this report

The remainder of this report is organized as follows. Chapter 2 provides a brief introduction to human auditory motion perception and acoustical time-to-contact. In Chapter 3 the details regarding the set of four experiments conducted for this study are described. Information regarding the purpose, methods and procedures, subjects and stimuli for each experiment is provided. Experimental results are presented in Chapter 4 while a discussion of the results follow in Chapter 5. Concluding remarks and future research directions are given in Chapter 6. Finally, detailed technical information regarding the equipment used in the experiments is provided in the Appendices.

## Chapter 2

# Background

This chapter reviews the primary auditory cues to motion. The majority of these cues are not necessarily specific to auditory motion but can also provide information with respect to static sound source localization and it is often the changes in static sound source localization cues from which we are able to extract motion information. This chapter ends with an introduction to acoustical time-to-contact, whereby auditory motion information is used to determine the time before a moving auditory source will make contact with an observer.

### 2.1 Auditory motion cues

We are capable of localizing dynamic sound sources, being just as sensitive to auditory velocity discrimination as we are with visual based velocity discrimination and are capable of making accurate auditory velocity judgments in time intervals as small as 30ms. However, the mechanisms responsible for this are not completely understood and the majority of sound localization research has focused on static environments where the sound source and listener are both stationary [40]. There is very little research available with respect to dynamic sound localization and little agreement on how the auditory systems encodes a moving sound source [16, 29, 43]. Furthermore, it is not completely clear whether the auditory system possesses special “auditory motion detectors” which respond solely to moving sounds. There is some evidence to support such a mechanism [37] and specific neural auditory motion detectors have been identified [3, 38]. There is also evidence supporting an alternate view in which the mechanisms that allow us to localize stationary sound sources are all that are required (and all we have) to detect moving sounds. This second model is known as the *snap-shot* hypothesis and under this model, a moving sound source is detected by comparing the location of the sound source at successive discrete times steps over some time interval [16, 37]. By integrating this snap-shot information over a period of time, the motion of the source is inferred [37]. Assuming the snap-shot hypothesis is correct, the velocity of a moving sound source cannot be determined directly, rather, velocity must be calculated using the total distance travelled by the sound source over the interval of interest and the time taken to travel this distance. Ericson [13] has shown that when considering a moving sound source, it is the total distance

travelled as opposed to actual speed of travel that is the cue to auditory motion, in agreement with the snap-shot hypothesis. However, the results of Lutfi and Wang [29] indicate that the dominant cue for motion discrimination is the speed of the moving sound source as opposed to the distance travelled. Other studies have also found velocity is important and can be detected rather than inferred (see [1, 53]). A further problem associated with the snap-shot hypothesis is its difficulty in accounting for our ability to discriminate between accelerating and decelerating auditory motion [37] since acceleration cannot be determined by simply comparing the time between the endpoints of the motion path [35]. Finally, studies have also shown that both a snap-shot and a neural mechanism may be used for auditory motion perception. According to a study conducted by Grantham [17], a neural mechanism can provide motion information for a restricted set of velocities while Carlile and Best [10] have shown we use both a direct neural mechanism and the snap-shot mechanism simultaneously when the corresponding cues are available.

Although the majority of auditory motion studies have focused primarily on constant velocity motion, a number of studies have investigated auditory motion with accelerating and decelerating moving sound sources. Perrott et al. [37] established that we are capable of determining whether a horizontally moving auditory source involves an acceleration or deceleration, being more accurate as both the acceleration and sound source duration is increased. Lutfi and Wang [29, 52] also investigated our ability to discriminate velocity and acceleration of horizontally moving sound sources using three acoustical cues: i) interaural time differences, ii) intensity and iii) Doppler frequency shifts (a description of these cues will follow). They found that we are capable of differentiating between velocity and acceleration. Their study also showed that at velocities of  $10\text{m}\cdot\text{s}^{-1}$ , intensity and interaural time differences are the pre-dominant cues for providing displacement information (e.g., information indicating the sound source has moved from its original position), while the Doppler frequency shifts are the predominant cues for velocity and acceleration discrimination.

Auditory distance and auditory motion perception are related to some degree. Auditory distance cues may also provide auditory motion cues. All static auditory distance cues can provide auditory motion information given the relative change in distance between the sound source and the observer. For example, when a sound source moves across the horizontal plane, the binaural cues (ITD and IID) will also change since the distance between the sound source and each of the ears changes as the source (or observer) moves. A systematic changing of the ITD cue is a reliable cue for the detection of a moving sound source provided the sound source does not lie on the median plane [40]. Although various aspects of an auditory stimulus can aid in the detection of auditory motion, Rosenblum et al. [40] identify the following cues as being most relevant for the detection of moving sound sources:

1. Intensity (sound level) changes.
2. Reverberation (ratio of direct-to-reverberant intensity).
3. Binaural cues (interaural time and intensity changes).
4. Doppler frequency shifts.

Although each of the cues listed above may provide motion information, intensity changes appear to be the dominant cue [40, 13] with some disagreement regarding the ordering of interaural temporal differences and frequency shifts. Ericson [13] concluded that Doppler frequency shifts dominate interaural temporal differences while Rosenblum et al. [40] found a reverse ordering. Greater details regarding the four auditory motion cues listed above and how they can signal self-motion are provided in the following sections.

**Intensity changes** Sound source intensity (a measure of energy propagated from the source per unit area and time) is inversely related to sound source distance. In other words, the intensity of the received sound is reduced as the sound source distance,  $r_s$ , increases (intensity increases with a decrease in sound source distance). Assuming an observer with a perfectly spherical head without any external ears (pinnae), the relationship between intensity and sound source distance follows the *inverse square law*. The change in intensity  $L$  (in decibels) at a receiver due to a change in sound source distance is [11]

$$L = 20 \times \log_{10} \left( \frac{r_s}{r_0} \right) \quad (2.1)$$

where  $r_0$  is the original source distance (e.g., reference distance). In other words, for each doubling of source distance, the intensity of the sound reaching the listener decreases by 6dB. Similarly, if the sound source distance is reduced by a factor of two, the intensity of the received sound will increase by 6dB. With respect to a moving sound source or moving observer, the intensity will increase or decrease continuously over time as the distance between the sound source and observer changes.

Although the inverse square law relates the physical intensity (sound level) of a sound to source distance, we perceive intensity as *loudness* [4, 57] and loudness is a subjective measure that cannot be measured directly. Loudness is not always an accurate representation of intensity [31] as the perceived loudness is frequency and bandwidth dependent [14, 32, 39]. Furthermore, the sound shadow of the head and the pinnae have an effect on the spectrum of the arriving sound.

**Reverberation** The collection of reflected sound reaching the listener varies with the geometry of the room relative to the listener [9] as well as the material of the room and the sound source frequency spectrum [15]. Reverberation provides a cue to sound source distance arising from changes in the ratio of the direct-to-reverberant intensity which varies with the sound source distance. As the sound source distance is increased, the intensity of the sound reaching a listener directly decreases, leading to a reduction in the ratio between the direct-to-reverberant intensities. Reverberation cues can provide absolute sound source distance estimation independent of overall sound source intensity [9, 11, 36]. As with the intensity cue, as the sound source or observer move, changes to the ratio of the direct-to-reverberant intensity provides a cue to motion.

**Binaural cues** Binaural cues include interaural time (ITD) and interaural intensity differences (IID) between the two ears and arise due to the fact that the two ears are separated by the head. Given this separation, unless the sound source lies on the median plane, the distance travelled by the sound waves emanating from the sound source to the listener’s left and right ear will differ. This causes the sound to reach the *ipsilateral* ear (the ear closest to the sound source) prior to reaching the *contralateral* ear (the ear farthest from the sound source). The difference in time between the arrival of the sound to each ear is known as the interaural time delay. ITD cues are relevant for localizing lower frequency sound (lower than approximately 1.5kHz). Similarly, given the separation of the ears by the head, when the wavelengths of a sound are short relative to the size of the head, the head will cast an “acoustical shadow”, attenuating the intensity of the sound reaching the contralateral ear [54]. This difference in sound level between the waves reaching the ipsilateral and contralateral ears is known as the interaural level difference.

Binaural cues are the predominant cues to localizing sound sources on the azimuthal plane [31]. As a sound source moves on the azimuthal plane, ITD and IID cues change continuously and as with the intensity and reverberation cues described above, this change provides a potential cue to auditory motion. When considering a sound source in the near field (e.g., within approximately one meter of the listener), the sound waves reaching the listener are spherical and the IID cues are in addition to direction, dependent on source distance [46, 51]. As a result, for a moving sound source in the near field, the changing IID cues over time may provide a cue to source motion for a source moving towards or away from the listener [7].

**Doppler frequency shifts** A stationary (omni-directional, mono-pole) sound source propagates uniformly in all directions. As the sound source moves, the wave crests “bunch up” (e.g., are brought closer together) in the direction of movement and are spread out in the opposite direction. As the waves crests are brought closer together, a decrease in wavelength results, while an increase in wavelength occurs in the opposite direction, where the waves are spread out. This change in wavelength  $\lambda$  is known as the *Doppler Effect* [55] and was first explained in 1842 by Christian Doppler. This shift in frequency can be very noticeable and has been shown to be a useful cue to locating moving auditory sources [24, 41].

Whether considering a moving or stationary sound source, the wave speed  $v_w$  (e.g., the distance travelled by a given point on the wave over some time interval), remains the same and is given by [55]:

$$v_w = \lambda f \tag{2.2}$$

where,  $\lambda$  is the wavelength and  $f$  is frequency of the sound waves emitted by the sound source. Since the wavelength of the sound waves generated by a moving sound source change, in order to maintain constant wave speed, the frequency must change. As the sound source approaches, the wavelength decreases (frequency is increased) and as the sound source recedes, the wavelength is increased (frequency is decreased).

## 2.2 Acoustical time-to-contact

An important aspect of detecting a moving sound source is the ability to determine the amount of time before the object emitting the sound makes contact with the observer [48]. We can use vision accurately to judge the time before an object within our visual field of view reaches us. The ability to determine the time in which an object, traveling with a constant velocity, will reach the observer is referred to as *optical time-to-contact* (denoted by the variable  $\tau_o$ ) and is the angular size  $\theta$  of the “image” on the retina divided by the rate of change of the image size at that particular time instant [20, 25, 26, 50]:

$$\tau_o = \frac{\theta}{d\theta/dt} \quad (2.3)$$

The expression for  $\tau_o$  given in Equation 2.3 is not necessarily restricted to image size and is valid for other stimuli which have an inverse relationship with distance [20]. Although visual time-to-contact has received a great deal of attention, a few studies have investigated *acoustical time-to-contact* ( $\tau_a$ ). According to Jenison [23], despite the physical differences between optics and acoustics, the meaning conveyed to an observer by a moving sound source is (within certain constraints) the same as a moving visual object. Whether it can be used as effectively as its visual counterpart remains to be answered. Studies have shown that subjects tend to under-estimate the arrival time of an approaching sound source [34, 42] and are nevertheless generally more accurate with judging visual time-to-contact [44]. However, Schiff and Oldack [44] have found that visually impaired subjects are just as accurate at using acoustical time-to-contact as sighted subjects are at using visual time-to-contact.

Although we can judge acoustical time-to-contact, it is not completely understood exactly how this is accomplished. Various cues are believed to play a role however their interaction remains unclear. A “generic” expression for acoustical time-to-contact is given as [45]

$$\tau_a = -\frac{r_s}{v_s} \quad (2.4)$$

where  $r_s$  is the distance between the observer and sound source and  $v_s = dr/dt$  is the velocity with which the sound source or observer is moving. As with the expression for optical time-to-contact  $\tau_o$  given by Equation 2.3, the ratio denoting acoustical time-to-contact  $\tau_a$  given by Equation 2.4 is not specified in terms of specific acoustic properties. Various acoustical cues are potential candidates provided that they have an (approximate) inverse relationship with distance. Such cues can include intensity, reverberation and sound source frequency spectrum [48].

### 2.2.1 Intensity based acoustical tau

Using intensity and the inverse square law, Shaw et al. [45] derived an expression for  $\tau_a$  based on the changing intensity of a sound generated by a sound source moving in a straight line

path towards an observer. Under these assumptions, acoustical time-to-contact  $\tau_a$  is given as

$$\tau = 2 \frac{kr_s^{-2}}{-2kr^{-3}v_s} \tag{2.5}$$

where,  $k$  is a constant,  $r_s$  is the distance between the sound source and observer, and  $v_s$  is the velocity of either the sound source or observer. This derivation ignores frequency effects despite the fact that a general analysis must account for frequency. In addition to these restrictions, as described by Stoffregen and Pittenger [48], there are several limitations to this derivation of  $\tau_a$  using intensity:

**Intermittent sound:** The ability to extract this intensity based information is largely dependent on the period with which the sound is continuous to the observer as it is difficult to draw any conclusions about  $\tau_a$  given brief intermittent sounds (most natural sounds are intermittent and not continuous).

**Silent observer:** The derivation assumes the sound generated by the sound source is the dominating sound in the environment. In other words, the intensity of any sounds generated by the observer or any other environmental sounds are irrelevant (e.g., the sound coming from the sound source will “mask” any other sounds or environmental noise).

**Prior knowledge of sound source intensity:** In order to make any use of intensity based  $\tau_a$ , prior knowledge of the absolute intensity of the sound source is required [18].

Lee et al. [27] describe the derivation of  $\tau_a$  based on reverberation (or more precisely, the ratio of direct-to-reverberant intensity) and its derivatives which eliminates the limitations inherent in the intensity based method presented by Shaw et al. [45]. An expression for  $\tau_a$  derived by differentiating frequency based distance information is provided by Stoffregen and Pittenger [48] and this also avoids many of the limitations inherent in the intensity based version of  $\tau_a$  of Shaw et al.

## 2.3 Summary

Although there is very little research available with respect to auditory motion perception, existing studies indicate the primary auditory motion cues include i) Doppler frequency shifts, ii) binaural cues iii) intensity changes and iv) reverberation. Intensity changes are often approximated by an inverse square law. Doppler frequency shifts are generated by the relative movement of a sound source and observer and do not exist when both are stationary. In contrast, intensity changes, binaural cues and reverberant properties are also relevant for static distance perception and sound localization but when considering a moving sound source (or moving observer) it is the changes over time with respect to these cues that provide auditory motion information. Although each of the cues listed above may provide motion information,



intensity changes appear to be the most dominant cue. In addition, similarly to visual time-to-contact, acoustical time-to-contact can provide information with respect to the time an acoustical object reaches us. Finally, the remainder of this report describes four experiments that examine our ability to judge the distance of self-motion when auditory and physical motion cues are presented independently or in combination. The results of these experiments provide greater insight to the role auditory information may play in the perception of self-motion.

## Chapter 3

# Experimental Method

### 3.1 Subjects

Subjects were unpaid volunteers and were either researchers, graduate students, professors or summer high school student assistants at York University. Subjects had normal or corrected-to-normal vision and no reported history of auditory or vestibular disease/disorders. In addition, none of the subjects reported any difficulties in hearing the stimulus or in completing any of the tasks. Twelve subjects participated in experiments one, two and three. The average age of the subjects was 27 years (range of 17 to 40 years). 10 subjects participated in experiment four, eight of whom also completed the other experiments (average age was 29 years with a range of 17 to 43 years). Prior to the start of the experiments, subjects were instructed of the required task by one of the experimenters. There was no training (“learning phase”) prior to any of the experiments. However, subjects were given several test trials to ensure they understood the tasks. Subjects were also instructed to sit in the chair with their back and head straight up and to keep their head stationary during each trial.

### 3.2 Equipment

#### 3.2.1 Subject motion cart and assembly

For experiments one, two and three, subjects sat on a wheeled cart (see Figures 3.1 and 3.2). Fixed in place next to the chair’s right arm-rest was the “subject response button” which was pressed by the subject to indicate they have reached the target (see Section 3.3), and hence completed a trial. Foam padding was placed on the chair, both on the seat and on the back-support as well as on the cart where the subject’s feet rested to limit the amount of vibration the subject felt (e.g., vibrations from the wheels that could provide a potential cue to motion). A “reference point” consisting of a large “X” was marked on the foam on the base of the cart at the front within the subject’s view. At the start of every trial, this reference point coincided with the “starting position”. All distance estimates were made relative to this marking. (See Appendix A for greater detail regarding the measurement of physical distance

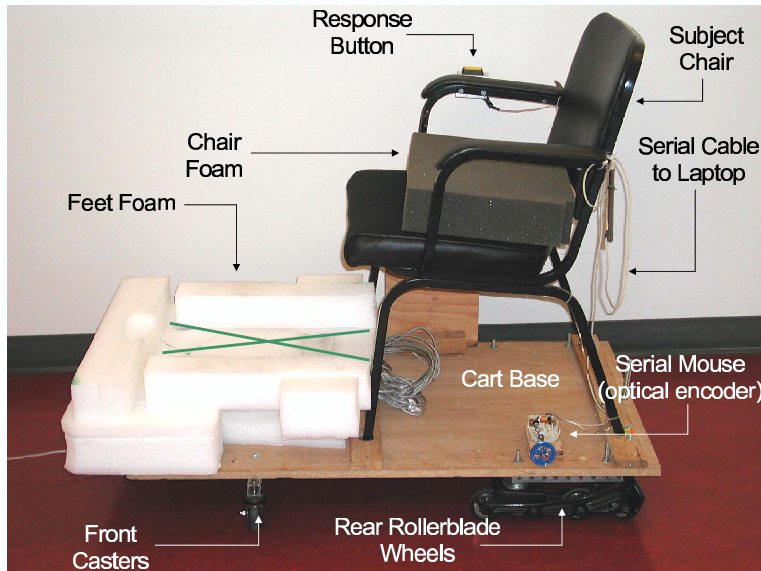


Figure 3.1: Subject motion cart used in experiments one, two and three.

moved.) To ensure that the cart followed a straight trajectory throughout its entire motion profile and did not veer from side-to-side, the cart was guided by a track affixed to the floor (see Appendix B).

### 3.2.2 Loudspeaker motion cart and assembly

For experiment four, a loudspeaker cart was constructed to move a sound source while the subject remained stationary. Loudspeakers were mounted on each of this cart's sides (Figure 3.3). The loudspeakers were placed facing each other a distance of 1m apart. As with the subject motion cart, this cart also followed the track on the floor.

### 3.2.3 Motor and motor controller

For the experiments involving physical motion (e.g., constant acceleration), the motion was generated with an EG & G MT-5330 servo motor mounted on a custom-built platform, controlled by a Galil DMC-630 motion controller and power amplifier. A steel cable connected the cart to the motor via a pulley assembly. A pulley assembly was used to convert the circular motion produced by the motor to linear motion thus allowing the cart to be moved linearly. A graphical illustration of the actual profiles is provided in Figure 3.4. The profiles were measured by having the subject motion cart (with one of the experimenters seated on it), follow each of the profiles for the entire 4m experimental span in addition to the two meters deceleration interval, while recording the accumulated distance at regular intervals (see Appendix A). The top, middle left, middle right, bottom left and bottom right graphs illustrate constant acceleration profiles for the acceleration rates of  $0.012\text{m}\cdot\text{s}^{-2}$ ,  $0.025\text{m}\cdot\text{s}^{-2}$ ,

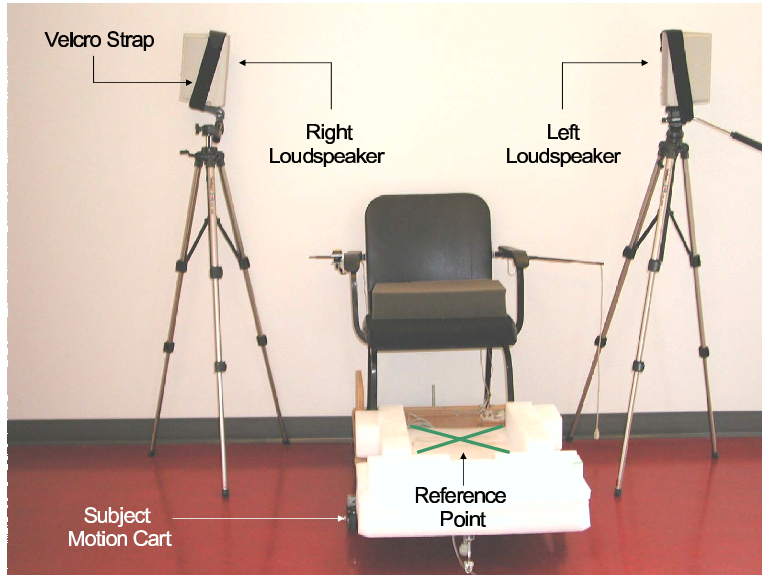


Figure 3.2: Subject motion cart and stationary sound sources (experiment one set-up).

$0.05\text{m}\cdot\text{s}^{-2}$ ,  $0.1\text{m}\cdot\text{s}^{-2}$ ,  $0.2\text{m}\cdot\text{s}^{-2}$  respectively. The x-axis of each of the large graphs represent time (in seconds) while the y-axis represents distance. The fixed line of each graph is the measured profile while the dotted line is the actual (ideal) profile. Close examination of both the actual and the ideal profiles reveals a maximum error of  $\pm 3\text{cm}$  for the first  $4\text{m}$  of the profile which corresponds to the experimental portion of the track. Included in the top left corner of each large graph is a sub-plot describing time (x-axis) versus estimated acceleration (y-axis).

### 3.2.4 Auditory stimuli

The auditory stimulus for each experiment consisted of a broadband, uniformly distributed, white-noise signal, sampled at a rate of  $44.1\text{kHz}$ . The noise was band-pass filtered using a 256-point Hamming windowed FIR filter with low and high frequency cut-offs of  $200\text{Hz}$  and  $10\text{kHz}$  respectively. A broadband signal was used as opposed to a single tone signal as sound source distance judgment is more accurate for broadband sound [34]. The increased accuracy in sound source distance judgments with the use of a broadband stimulus may be a direct consequence of the increasing attenuation of the higher frequency components of a propagating sound [4, 11, 33, 36]. In order to ensure the subject did not learn to associate the sound level with a particular target distance or acceleration profile, the level of the sound stimulus was randomly chosen from one of three different initial levels for each presentation ( $66\text{dB}$ ,  $69\text{dB}$  and  $72\text{dB}$ ), measured with a Radio Shack sound level meter (model 33 – 2055) with an A-weighting, placed directly at the starting position where the subject's head would be and averaged over a  $15\text{s}$  duration. All auditory stimuli were played through a pair of

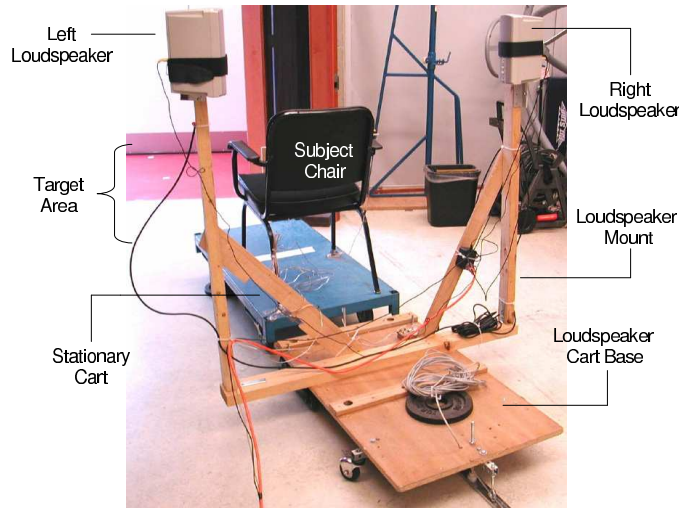


Figure 3.3: Loudspeaker motion cart used in experiment four.

Distance (m)	Minimum Level (dB)	Maximum Level (dB)	Average Level (dB)
1	67	71	68
2	65	68	66
3	64	69	65
4	62	65	63

Table 3.1: Auditory stimuli sound levels at each of the four target distances. Sound level one: 72dB. Measured by averaging the response of an A-weighted sound level meter for 15 seconds.

Yamaha YST-M15 loudspeakers.

In addition to measuring the sound level at the starting position, it was also measured (for each of the three reference sound levels), at each of the target distances of 1m, 2m, 3m and 4m, once again, time averaged over 15 seconds using the A-weighting on the sound level meter. A summary of the measured levels at each of the four target distances is provided for each of the three sound levels of 72dB, 69dB and 66dB in Tables 3.1, 3.2 and 3.3 respectively. On average, for each doubling of sound source distance (e.g., from 1m to 2m and from 2m to 4m), a decrease of 2.7dB occurred.

### Background noise

The background noise level was measured in the absence of the sound stimulus. Measurements were averaged over a 15s interval using the A-weighting sound level meter. Measurements

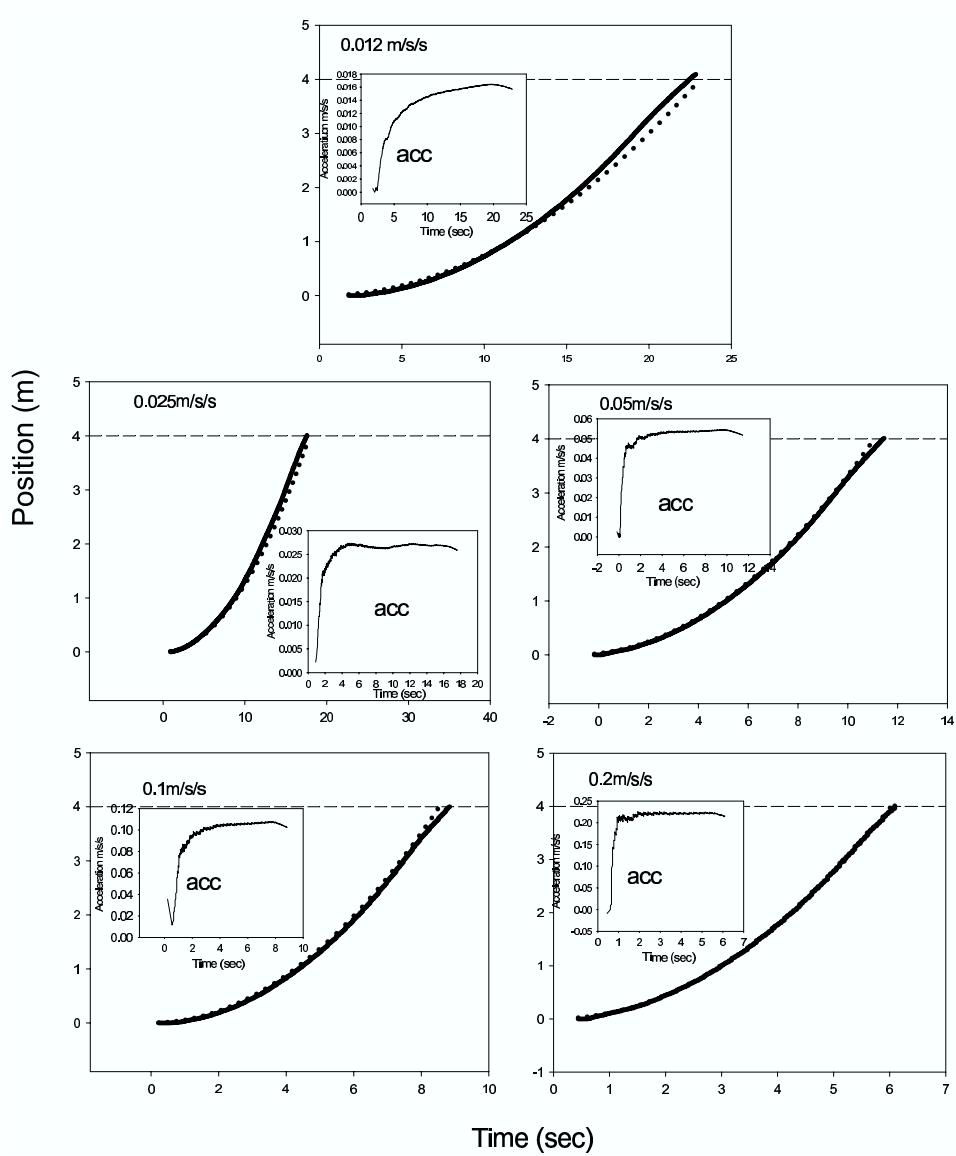


Figure 3.4: Acceleration motion profiles generated by the motor. Top, middle left, middle right, bottom left and bottom right graphs illustrates the constant acceleration profiles for the acceleration rates of  $0.012\text{m}\cdot\text{s}^{-2}$ ,  $0.025\text{m}\cdot\text{s}^{-2}$ ,  $0.05\text{m}\cdot\text{s}^{-2}$ ,  $0.1\text{m}\cdot\text{s}^{-2}$ ,  $0.2\text{m}\cdot\text{s}^{-2}$  respectively.

Distance (m)	Minimum Level (dB)	Maximum Level (dB)	Average Level (dB)
1	66	68	67
2	64	66	65
3	63	65	64
4	62	65	62

Table 3.2: Auditory stimuli sound levels at each of the four target distances. Sound level two: 69dB. Measured by averaging the response of an A-weighted sound level meter for 15 seconds.

Distance (m)	Minimum Level (dB)	Maximum Level (dB)	Average Level (dB)
1	63	64	63
2	60	63	60
3	55	64	56
4	57	61	57

Table 3.3: Auditory stimuli sound levels at each of the four target distances. Sound level three: 66dB. Measured by averaging the response of an A-weighted sound level meter for 15 seconds.

were made at the starting position and at each of the four target distances. The average background sound levels at each target distance and at the starting position was below 50dB (the minimum sound level measurable with the sound level meter) with a maximum level of 57dB. In addition to these static measurements, background noise levels were also measured while moving with the cart through one of the acceleration profiles (the  $0.012\text{m}\cdot\text{s}^{-2}$  acceleration profile). The average sound level was 54dB with maximum and minimum values of 56dB and 51dB respectively. Background levels were far below the levels encountered in the presence of the sound stimulus.

### 3.3 Experimental procedure

In all four experiments, each subject was presented with a large  $1.5\text{m} \times 1.0\text{m}$ , brightly colored “T”-shaped physical target at one of four pre-defined distances (1m, 2m, 3m or 4m) in front of them. The large size of the target, along with its bright color, made it extremely easy to see. The target was held in place by one of the experimenters (see Figure 3.5). Subjects were allowed to view the target for as long as necessary (typically under 30 seconds) and were also encouraged to move their head from side-to-side to obtain parallax cues in addition to static cues such as size and disparity cues, to the target’s distance. Subjects were then blindfolded and presented with the stimulus. In experiment one (“physical motion only” or “MO”) the only stimulus presented to the subjects was physical motion which was achieved by

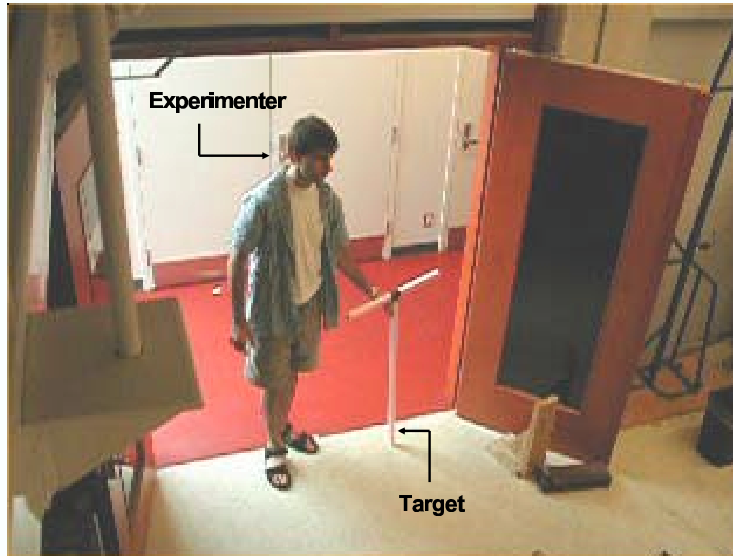


Figure 3.5: Experimenter holding the physical target.

physically moving the subjects some pre-defined distance. Subjects were also presented with a single modality stimulus in experiment two (“simulated auditory motion only” or “AO”) however, the stimulus consisted of an auditory signal whose level was decreased while the subject remained stationary. In experiment three (“physical motion + auditory motion” or “A+M”), the subject was moved physically in the presence of a stationary auditory source and in experiment four (“physically moving audio” or “MA”), a moving auditory stimulus was presented while the subject remained stationary. Once the trial began the subject indicated when they had perceived that they had reached the previously viewed target by pressing the response button. Pressing the button ended the trial and any auditory stimulus or physical motion was stopped. When a trial included physical motion, after coming to a stop, the cart was physically pushed back to its original starting position by one of the experimenters.

In experiments one, three and four which included physical motion, either the subject or the sound source was moved following one of five rates of acceleration ( $0.012\text{m}\cdot\text{s}^{-2}$ ,  $0.025\text{m}\cdot\text{s}^{-2}$ ,  $0.05\text{m}\cdot\text{s}^{-2}$ ,  $0.1\text{m}\cdot\text{s}^{-2}$  or  $0.2\text{m}\cdot\text{s}^{-2}$ ). The acceleration profile of  $0.012\text{m}\cdot\text{s}^{-2}$  was chosen since it is below the reported vestibular threshold of  $0.05\text{m}\cdot\text{s}^{-2}$  [8]. Each acceleration profile was repeated for target distances of 1m, 2m, 3m and 4m. Conditions were presented in a random order. The trials of experiments one, two and three each consisted of 20 trials. The trials of each of these experiments were randomly interleaved and carried out as a single experiment by all participants. The trials of experiment four also consisted of 20 trials however experiment four was conducted separately.



### 3.3.1 Experiment one: physical motion only

This experiment examined the perception of self-motion using the physical motion cue only. No auditory cues were present in this experiment. The subject was seated on the motion cart that was pulled by the motor following one of the pre-defined acceleration profiles. Subjects pressed the subject response button when they perceived that they (the X reference point marked on the cart) had reached the target.

### 3.3.2 Experiment two: simulated auditory motion only

This experiment investigated whether the reduction of sound intensity (sound level) alone can be used as a reliable cue for self-motion perception. There was no physical motion of either the subject or the loudspeakers in this experiment. Rather, the level of the auditory stimulus was decreased to imitate the reduction in intensity which would occur if the subject was actually accelerating away from the sound source at one of the five rates of acceleration used in experiments two, three and four. The sound signal at time  $t$ , ( $s_d^t$ ) was computed as

$$s_d^t = \frac{s_o}{r_s^t} \quad (3.1)$$

where,  $s_o$  is the original, uniformly distributed sound signal (see Section 3.2.4) and  $r_s^t$  is the distance between the sound source and the observer at time  $t$ , computed as

$$r_s^t = \frac{1}{2} \times at^2, \quad (3.2)$$

where,  $a$  is acceleration (one of either  $0.012\text{m.s}^{-2}$ ,  $0.025\text{m.s}^{-2}$ ,  $0.05\text{m.s}^{-2}$ ,  $0.1\text{m.s}^{-2}$  or  $0.2\text{m.s}^{-2}$ ),  $t$  is time. Although this experiment did not include any physical motion, just before the stimulus was presented, the motor was started (powered “ON”) by one of the experimenters. The motor was powered ON to ensure the subject did not learn to associate the noise associated with powering the motor ON with physical motion. Subjects were told to press the subject response button when they perceived the reference point on the cart to have reached the target.

### 3.3.3 Experiment three: physical motion + auditory motion

The sound source was placed at the starting position and remained stationary while the subject was accelerated towards the target. The purpose of this experiment was to examine whether any acoustical properties associated with increasing the distance to a sound source (most notably a decrease in intensity and a decrease in the ratio of direct-to-reverberant intensity) had any effect on the perception of linear self-motion.

Each loudspeaker was mounted on an adjustable height camera tripod (Figure 3.2). The height of the loudspeakers was set equal to the height of the subject’s ears while seated

on the cart and the two loudspeakers were separated by one meter. Once the subject was comfortable with the visual target's position, they were blindfolded and the auditory stimulus were presented, followed by physical motion. When the subject pressed the subject response button, indicating they perceived that they had reached the target distance, the cart was stopped and physically pushed back to its original starting position. The time between when the subject pressed the button (to indicate they reached the target) and when the auditory stimulus and physical motion came to a stop varied by a few seconds. Varying this time was done to limit the use of any potential cues the subject may have received while being physically returned to the starting position. As with experiment one, distances were estimated relative to the X-shaped reference point on the subject motion cart.

### **3.3.4 Experiment four: physically moving audio**

In this experiment, the subject remained stationary at the starting position while seated on the stationary subject cart. The sound source (loudspeakers) was mounted on the loudspeaker cart which was placed just behind the listener (Figure 3.3). Rather than having the subject move away from the sound source as in experiment two, the cart (and therefore the sound source) was accelerated away from the stationary subject following one of the five acceleration profiles used in the other experiments.

As shown in Figure 3.3, a stationary subject cart was placed in front of the loudspeaker cart. Subjects indicated they reached the target by pressing the response button located on the right chair handle. An X-shaped reference marker was also placed on the stationary subject cart, marking the reference point as with the earlier experiments. Subjects indicated when they had reached the target by pressing the response button.

# Chapter 4

## Results

For each condition, the subject's perceived (target) distance was measured and compared to the actual or simulated distance travelled (actual distance). A summary of the perceived target distance versus the actual target distance (including standard error) for each of the five accelerations for each experimental condition is provided in Figure 4.1. The ratio of perceived target distance and the actual distance is called *perceptual gain*, denoted by  $g_p$  [19]

$$g_p = \frac{d_p}{d_a} \quad (4.1)$$

where,  $d_a$  is the actual distance moved and  $d_p$  is the subject's perceived distance. As shown in Figure 4.2 the perceptual gain is calculated by taking the inverse of the resulting slope of the line between target distance versus actual distance. Perceptual gains were averaged across subjects for each condition and for each experiment. When the perceived distance equals the actual distance ( $d_p = d_a$ ), the perceptual gain is unity. A perceptual gain greater than one results when the perceived distance is greater than the actual distance when subjects over-estimate the distance they have travelled. Conversely, a perceptual gain of less than one occurs when the perceived distance is less than the actual distance and subjects underestimate the distance travelled.

A graphical representation of the resulting perceptual gains as a function of acceleration for each of the four experiments is given in Figure 4.3. In each experiment, the perceptual gain for each acceleration was averaged across all subjects who participated in the experiment. The horizontal dashed line represents a perceptual gain of one. Summaries of the perceptual gains and corresponding standard error for each acceleration for experiments one, two, three and four are provided in Tables 4.1, 4.2, 4.3 and 4.4 respectively.

### 4.1 Experiment one: physical motion only

Averaged perceptual gain values for motion only conditions by acceleration are shown as filled circles in Figure 4.3. Perceptual gain responses varied systematically with acceleration

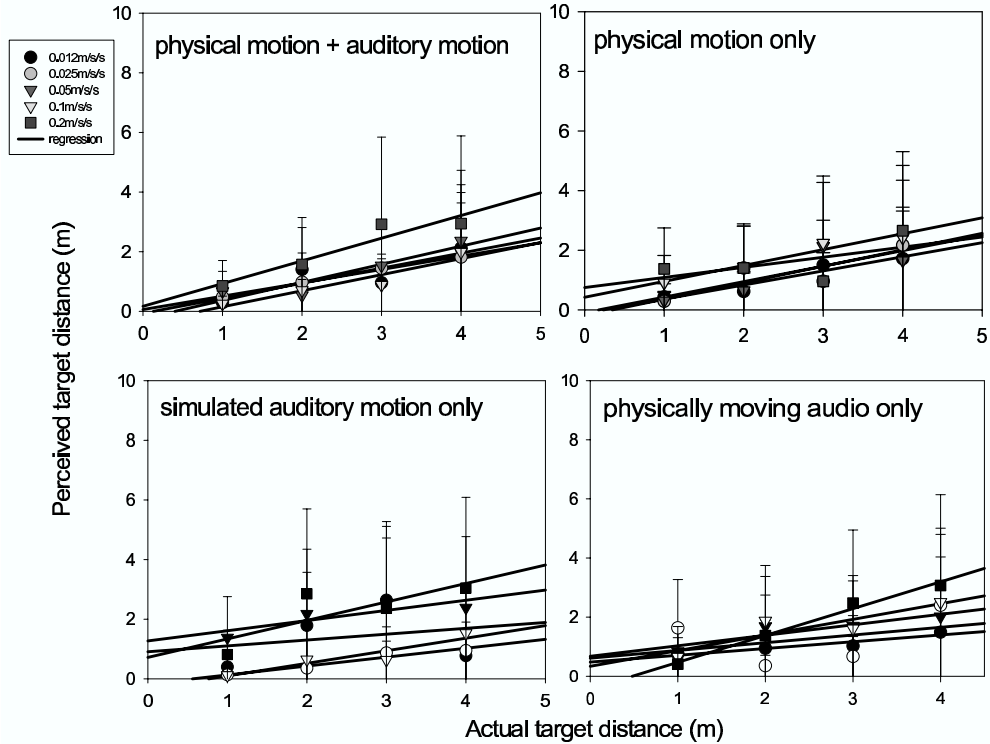


Figure 4.1: Target distance versus response distance for each acceleration of each experimental condition. The inverse of the slope of the linear fit to each condition is the perceptual gain.

with low accelerations producing a relatively low mean perceptual gain (2.0) and higher accelerations producing a higher mean perceptual gain (3.0) (see Table 1).

## 4.2 Experiment two: simulated auditory motion only

Averaged perceptual gain values for simulated auditory motion only conditions by acceleration are shown as open circles in Figure 4.3. This condition produced the highest averaged perceptual gain response (perceptual gain 5.0 at  $0.012\text{m}\cdot\text{s}^{-2}$ ) which systematically decreased with acceleration to a perceptual gain of 1.6 at  $0.2\text{m}\cdot\text{s}^{-2}$  (see Table 2).

## 4.3 Experiment three: physical motion + auditory motion

Responses to the combined physical motion and physically moving auditory motion condition are shown in Figure 4.3 as grey squares. Averaged perceptual gain responses were approximately 1.8 and were consistent across accelerations reaching a low of 1.3 at  $0.2\text{m}\cdot\text{s}^{-2}$  (see Table 3).

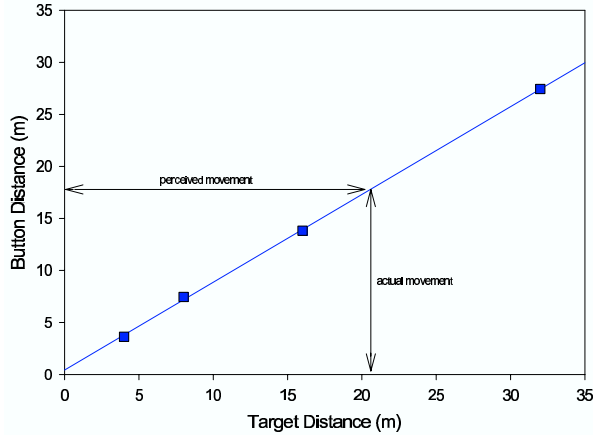


Figure 4.2: Example of perceptual gain which is defined as the ratio of perceived movement (target distance) to actual movement (button distance). Perceptual gain is therefore the reciprocal of the slope shown.

Acceleration ( $\text{m.s}^{-2}$ )	Perceptual Gain ( $g_p$ )
0.012	$2.11 \pm 0.27$
0.025	$1.93 \pm 0.25$
0.05	$1.81 \pm 0.24$
0.1	$1.88 \pm 0.26$
0.2	$2.95 \pm 0.11$

Table 4.1: Average perceptual gains for each acceleration of experiment one (physical motion only).

#### 4.4 Experiment four: physically moving audio

Physically moving audio conditions are presented as dark squares in Figure 4.3. The physically moving audio condition closely resembles the averaged responses of the simulated moving auditory motion where low accelerations produced high perceptual gains (4.4) and dropped systematically with acceleration reaching a low of 1.3 at  $0.2\text{m.s}^{-2}$  (see Table 4).

#### 4.5 Effects of condition

A repeated measures ANOVA was performed on the mean perceptual gains obtained for each condition for each subject. There was a main effect for condition ( $\mathbf{F}(3, 40) = 10.22$ ,  $p < 0.001$ ). A Post-hoc multiple comparison was performed to compare all pairwise differences

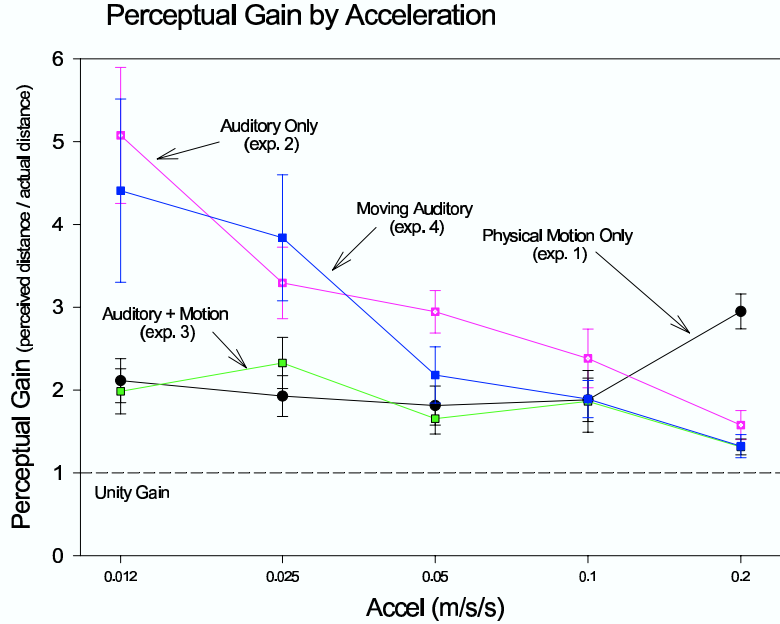


Figure 4.3: Summary of experimental results: perceptual gain (perceived distance / actual distance) as a function of acceleration (on log axis) for experiments one, two, three and four.

within conditions and is shown in Table 4.5. In this table, the first column denotes acceleration while columns two, three, four and five denote the four experimental conditions. The entries of columns two, three, four and five denote which of the five accelerations were statistically different when considering each experimental condition individually.

Post-hoc tests were also performed to determine which conditions differed between conditions by acceleration. Table 4.6 summarizes the statistical differences between experimental conditions by acceleration. As with Table 4.5, the first column denotes acceleration while columns two, three, four and five denote the four experimental conditions. The entries of columns two, three, four and five denote, for each of the accelerations in column one, which conditions and acceleration (considered together) differ statistically.

## 4.6 Effect of acceleration

A repeated measures ANOVA test and post-hoc comparison test were also performed on the five different accelerations. Results of the ANOVA test confirm a significant difference between accelerations ( $F(4, 40) = 9.78, p < 0.01$ ). According to these tests, the accelerations can be divided into two groups labeled slow and fast, where the slow accelerations are  $0.012\text{m}\cdot\text{s}^{-2}$ ,  $0.025\text{m}\cdot\text{s}^{-2}$  and  $0.05\text{m}\cdot\text{s}^{-2}$  and the fast accelerations are  $0.1\text{m}\cdot\text{s}^{-2}$  and  $0.2\text{m}\cdot\text{s}^{-2}$ .

Acceleration (m.s <sup>-2</sup> )	Perceptual Gain ( $g_p$ )
0.012	5.08 ±0.82
0.025	3.29 ±0.43
0.05	2.95 ±0.26
0.1	2.38 ±0.35
0.2	1.58 ±0.18

Table 4.2: Average perceptual gains for each acceleration of experiment two (simulated auditory motion only).

Acceleration (m.s <sup>-2</sup> )	Perceptual Gain ( $g_p$ )
0.012	1.98 ±0.27
0.025	2.33 ±0.31
0.05	1.65 ±0.19
0.1	1.86 ±0.19
0.2	1.31 ±0.10

Table 4.3: Average perceptual gain for each acceleration of experiment three (physical motion + auditory motion).

Slow acceleration conditions showed a significant difference between the conditions.

Acceleration (m.s <sup>-2</sup> )	Perceptual Gain ( $g_p$ )
0.012	4.40 ±1.1
0.025	3.84 ±0.76
0.05	2.18 ±0.34
0.1	1.89 ±0.22
0.2	1.32 ±0.14

Table 4.4: Average perceptual gain for each acceleration of experiment four (physically moving audio).

<b>Accel.</b>	<b>(MO)</b>	<b>(AO)</b>	<b>(A+M)</b>	<b>(MV)</b>
<b>0.012</b>	-	0.05, 0.1, 0.2	-	-
<b>0.025</b>	-	-	-	0.1, 0.2
<b>0.05</b>	-	0.012	-	-
<b>0.1</b>	-	0.012	-	-
<b>0.2</b>	-	0.012	-	-

Table 4.5: Tukey-Kramer multiple-comparison test for differences within conditions by acceleration.

<b>Accel.</b>	<b>(MO)</b>	<b>(AO)</b>
0.012	(MA: 0.025), (AO: 0.012) (A+M: 0.2), (MA: 0.05), (MA: 0.025), (AO: 0.012) (A+M: 0.2)	(A+M: 0.2), (MA: 0.05),
0.025	(MA: 0.025), (AO: 0.012)	(A+M: 0.2)
0.05	(MA: 0.025), (AO: 0.012)	-
0.1	(MA: 0.025), (AO: 0.012)	(AO: 0.012), (MA: 0.025)
0.2	0.2 (AO: 0.012)	(MA: 0.025)
<b>Accel.</b>	<b>(A+M)</b>	<b>(MA)</b>
0.012	(MA: 0.025), (AO: 0.012)	(A+M: 0.2)
0.025	(AO: 0.012), (MO: 0.012, 0.025, 0.05, 0.1)	(A+M: 0.012, 0.05, 0.1, 0.2), (AO: 0.2)
0.05	(MA: 0.025), (AO: 0.012)	(AO: 0.012)
0.1	-	(AO: 0.012)
0.2	(AO: 0.012, 0.025), (MA 0.012, 0.025)	(AO: 0.012)

Table 4.6: Tukey-Kramer multiple-comparison test for differences between conditions by acceleration.



# Chapter 5

## Discussion

### 5.1 Experiment one: physical motion only

In this experiment, physical motion was the only stimulus provided to the subjects. Consistent with previous studies (e.g., [19, 22, 30]) the results of this experiment indicate physical motion is often overestimated. Systematic variation of perceptual gain with accelerations for each of the five accelerations was observed with responses reaching their highest (mean perceptual gain of 3) for the acceleration of  $0.2\text{m}\cdot\text{s}^{-2}$ . Curiously, high perceptual gain responses, representing overestimation of motion, were observed at accelerations below the vestibular threshold.

Harris et al. [19] had subjects match physical motion to physical motion targets using one profile for the target and a faster or slower profile for the trial. These results show that subjects can use sensory information associated with physical motion (e.g., vestibular and/or cutaneous cues) without vision. Here, subjects appear to be able to utilize physical motion cues at an acceleration below the vestibular threshold. Although there should be no vestibular cues when moving at a rate of acceleration below the vestibular threshold, other potential cues to self-motion may be available in the experiment. In particular, the vibrations which arise as the cart is moving could provide information in the form of vibration (tactile) cues. Care was taken to ensure these cues were limited. In particular, the chair the subjects were seated on was padded with foam, and foam was also placed on the base of the subject motion cart where the subjects placed their feet on. Other cues could include the initial “jerk” component of the motion profile experienced when the motion first begins [5], wind striking the faces of the subjects during the motion (as reported by several of the subjects) and noise present in the environment as well as any noise produced by the moving cart itself. Although the initial “jerk” could not be removed, it was limited by ensuring the cable pulling the cart was kept under constant tension.

## 5.2 Experiment two: simulated auditory motion only

In this experiment both the subject and the sound source remained stationary while the intensity of the sound source was decreased to imitate the decrease in intensity which would have occurred had the subject accelerated away from a stationary sound source. No other acoustical cues associated with a moving sound source were available (e.g., reverberation and therefore the ratio of direct-to-reverberant intensity, binaural cues, changing spectrum cues etc.). The estimation of sound source distance using sound source intensity information alone resulted in a large perceptual gain (see Figure 4.3). This finding is consistent with previous studies involving static sound source distance estimation [57].

The authors are not aware of any studies examining linear self-motion perception in the presence of accelerating auditory cues only. Several studies are available which have examined self-motion (constant velocity) with respect to a stationary (reference) sound source (e.g., see [2, 34]), and have also found subjects over-estimate their self-motion or alternatively, underestimate the distance to the stationary sound source.

As shown in Figure 4.3, the perceptual gains decrease as the acceleration increases and as described in Section 4, this change is significant, indicating accuracy does improve as acceleration is increased. This result does verify the conclusions reached by Perrott et al. [37] who examined the ability of subjects to discriminate between horizontally moving sound sources that were either accelerating or decelerating. They conclude that we are capable of determining whether a horizontally moving auditory source involved an acceleration or deceleration, with increasing accuracy as acceleration is increased.

## 5.3 Experiment three: physical motion + auditory motion

In this experiment, the physical motion and auditory stimuli were combined. The auditory stimulus consisted of a uniformly distributed random noise signal output through a pair of two stationary loudspeakers placed at the starting position. As the subject was accelerated towards the target, the loudness of the sound decreased since the distance between the subject and sound source increased.

This condition was significantly different than the other three conditions suggesting that information from more modalities results in more accurate performance. These results indicate the addition of the motion (vestibular) cue does make the task of self-motion judgment more accurate as opposed to using decreasing sound intensity alone. According to Wuerger et al. [56] there is physiological and behavioral evidence indicating that the integration of multi-sensory information is more likely to provide more accurate information, especially when the single modalities are individually close to threshold (see also [47]).

## 5.4 Experiment four: physically moving audio

In this experiment, rather than changing the intensity (level) of the auditory signal to simulate the subject moving away from the sound source, the sound source (loudspeakers) were

physically moved away from the subject. As with the other experiments, an over-estimation of the subjects self-motion perception resulted. The major difference in the results of this experiment is that the other cues associated with a moving sound source (e.g., reverberation etc.), would be available, thereby potentially resulting in improved performance. The results from this experiment and experiment two (simulated auditory motion only) were not significantly different. These results differ from studies which have found reverberation cues to play a significant role in sound source distance estimation. [9, 11, 36]. However the room itself in which the experiment took place was large, measuring  $12\text{m} \times 25\text{m}$  and the energy of any reflections reaching the subject may have been too weak and could have been masked by the auditory stimulus itself. As with experiment two in which the only stimulus presented was auditory and as found by Perrott et al. [37], accuracy in this experiment increased with increasing acceleration. The over-estimation of self-motion as a sound source is physically moved away has also been examined by Neuhoff [34] who also found subjects did over-estimate their self-motion and that this over-estimation was greater when considering an approaching sound source as opposed to a receding one.

## Chapter 6

# Conclusions

The majority of the research effort examining self-motion perception has concentrated on the visual and vestibular senses. Although vision plays a critical role the understanding of our surroundings and a large portion of the brain is dedicated to visual processing, it is certainly not the only cue available to us and at times it cannot be used (e.g., in the dark or for objects which are not within our visual field of view). Furthermore, the integration of multi-sensory information is more likely to provide more accurate information, as opposed to a single modality. In contrast to the visual system, the auditory system is omni-directional and can function in the dark and in other situations where vision is restricted (e.g., fog, heavy snow).

In this study, a series of four experiments were conducted to examine the role of auditory cues for self-motion perception, when used alone or in conjunction with physical motion cues. Self-motion estimation was most accurate when both vestibular and auditory cues were made available simultaneously and with respect to simulated auditory motion cues, accuracy of motion estimation increased with increasing acceleration. These results conform with the majority of existing research which has examined auditory motion perception (e.g., [29, 37]). A finding which deserves further attention is the observation that performance was the same for the “simulated auditory motion only” and “physically moving audio” conditions. Although reverberation has been shown to play a critical role in auditory distance perception, this was not observed here. Future work will include repeating these two conditions in a smaller enclosure, either by using a smaller room or by separating the existing room with some type of “room dividers” or by simulating reverberation in static auditory experiments.

These experiments have demonstrated for the first time the very significant contribution of auditory cues to the determination of the perception of self-motion. As demonstrated in previous studies and as verified in this study, physical self-motion in the dark is usually associated with very large perceptual gains. The experiments described here demonstrate that the addition of auditory cues contribute significantly to the accuracy of perceived self-motion.

The visual system does not seem to improve the vestibular system’s apparently poor estimation of self-motion distance [19]. The vestibular system seems to dominate the visual system such that high perceptual gains are still found even when vision is available (see

[19]). Sound, unexpectedly, seems to be much more effective in making perceived self-motion accurate, particularly at higher accelerations. At lower accelerations, the vestibular system is dominant.

# Appendix A

## Accurate measure of physical motion

In this appendix greater information, including technical details, will be provided regarding the distance recording equipment. When considering the three experiments that contained physical motion, the distance travelled was accurately measured using the optical encoders of an appropriately modified, standard PC serial (RS-232-C) mouse, earth fixed wire and laptop PC.

### A.1 Distance recording equipment

As previously described in Chapter 3, in each trial of all the experiments, a measure of the distance travelled by the subject seated on the motion cart, from the starting position to the target, was required. Three of the four experiments (experiments one, three and four) involved physical motion of either the subject motion cart or the loudspeaker motion cart while in experiment two the subject remained stationary and judged the distance travelled based on a stationary auditory stimulus with decreasing level. In experiment two, there was no physical motion but rather, the level of an auditory stimulus was decreased to imitate the reduction of sound level which would occur if the motion cart (and hence subject) was actually moved following one the pre-defined acceleration profiles. Since the rate of acceleration was known, by recording the time taken between the onset of the auditory stimulus and the time the subject indicated they reached the target, the total distance travelled for each trial of experiment two was calculated as follows:

$$d_t = \frac{1}{2}at^2 \tag{A.1}$$

where  $d_t$  is the distance from the starting position to the position corresponding to the time the subject pressed the button to indicate they reached the target,  $a$  is acceleration (e.g., one

of  $0.012\text{m.s}^{-2}$ ,  $0.025\text{m.s}^{-2}$ ,  $0.05\text{m.s}^{-2}$ ,  $0.1\text{m.s}^{-2}$  or  $0.2\text{m.s}^{-2}$ ) and  $t$  is the time from the onset of the auditory stimulus until the perceived target is reached (e.g., the response button is pressed).

A modified two-button Microsoft serial mouse and “earth-fixed” wire were used to record the distance travelled for the trials of the experiments involving physical motion. A mouse contains two optical encoders to record distance, one for each of the X and Y axis and is used to convert hand motions into signals the computer can use and make sense of. As described in the following sections, mice are very accurate (high resolution), capable of detecting very small movements and updating at a high rate. Furthermore, when considering a serial mouse, the converted motion signals are transferred to a PC using a standard serial (RS-232) connection, making it extremely simple for communications between an application to take place. These factors, along with the fact that serial mice are readily available and economical have made them attractive for many applications requiring accurate motion detection including the control of optical telescopes.

### A.1.1 Mouse operation

The majority of mechanical and optical-mechanical mice contain a ball inside the mouse which touches the desktop (or any other surface) and rotates as the mouse is moved. Referring to Figure A.1, two rollers inside the mouse, oriented perpendicularly to each other, make contact with the ball. As the ball moves, depending on the direction of its movement, one or both of the rollers rotate as well (e.g., if the ball is rotated along either the X or Y axis solely then only the roller corresponding to the X or Y axis will rotate and if the ball is moved diagonally, then both rollers will rotate). The rollers are each connected to their own shaft and on the other end of each shaft is a disk with evenly spaced rectangular slots in it. Rotation of the roller will result (via the shaft), in a rotation of the disk. As shown in Figure A.2, the disk of each shaft is placed between two light emitting diodes (LEDs) and two “light sensitive transistors”. Each LED continuously shines light which is collected by its corresponding transistor. However, since the disk contains these spaced slots, light from the LED will reach the transistor only through these slots and is blocked otherwise. In other words, light is “pulsed” through these slots and the transistor will detect these light pulses. The pulse rate is directly related to both the speed of the mouse movement and the distance travelled [6]. The information (pulses) from the transistors are then processed by the mouse controller and delivered to the PC. When considering a serial mouse, the transistor information is converted to RS-232 compatible signals and transferred to the PC via a serial connection. A single LED transistor pair would suffice to detect the pulses and hence mouse motion without any regards to the direction of motion. However using two LED/transistor pairs allows for the detection of the direction of disk rotation (and hence mouse rotation) to be determined. Further details regarding this direction detection capability is provided in [6].

Greater details regarding the modifications made to enable the use of a two-button Microsoft serial mouse to record distance travelled in the Experiments is provided in the following section while Section A.1.2 describes the Microsoft serial mouse protocol.

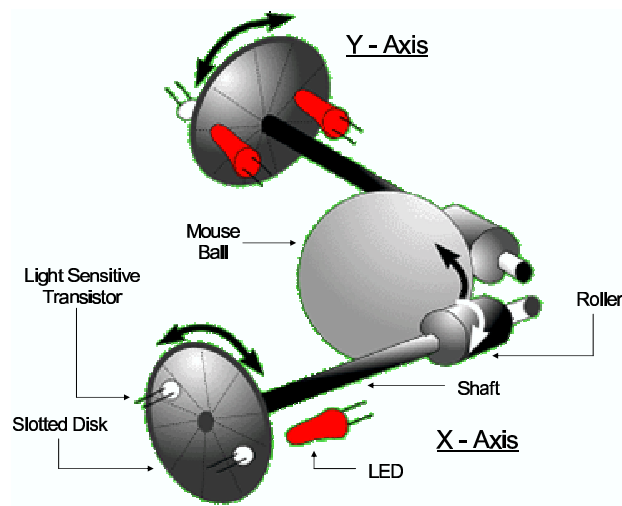


Figure A.1: Main components allowing a mouse to detect motion. As the mouse ball is moved, it may cause one or both of the rollers to turn. The turning rollers cause the mouse shaft to rotate which in turn leads to the rotation of the slotted disk (the slots are not shown in this diagram). The light emitting diodes (LEDs) emit light which is captured by their corresponding light sensitive transistors only when the light passes through one of the slots. The rate at which the disk spins is directly related to the rate the light is captured and hence mouse speed and distance moved.



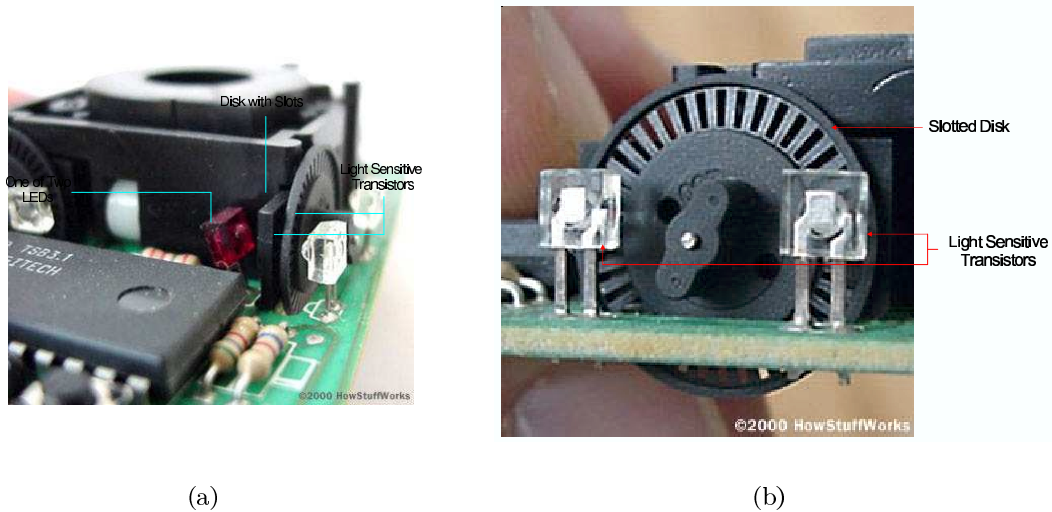
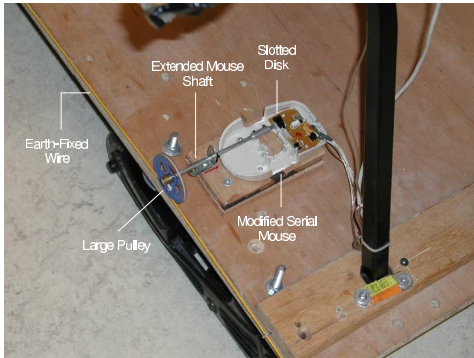


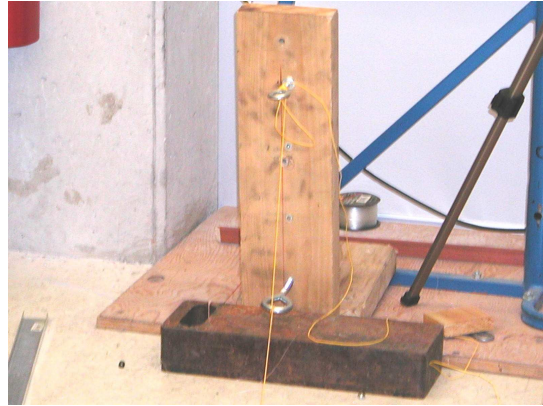
Figure A.2: Two views of the mouse encoder. The slotted wheel is placed between two LEDs and two corresponding light sensitive transistors. The light emitted by each LED is captured by its corresponding transistor only when the light passes through one of the slots of the disk.

### A.1.2 Modifying the serial mouse for use in these experiments

In order to record the distance travelled by the cart in the experiments, rather than using the mouse ball to rotate the rollers, shaft and disk assembly, as shown in Figure A.3, a pulley attached to the encoder shaft, moving along an “earth-fixed” wire was used instead. The mouse was mounted to the cart in such a manner so the pulley “cleared” the cart, hanging just over the side of the cart. Running parallel to the track, for the complete length of the track and at approximately the same height off the ground as the pulley, was a wire (fishing line) which was permanently fixed at each end. As illustrated in Figure A.3, the wire made a loop through the pulley which caused the pulley to rotate as the cart was moved from its starting position to the target. The rotating pulley caused the shaft to turn which then caused the disk to rotate, ultimately leading to the light pulses previously described (e.g., the pulley replaced the mouse ball). The amount of rotation and hence the rate of light pulses, is inversely proportional to the size of the pulley (e.g., increasing the size of the pulley decreases the speed of shaft rotation and hence rate of light pulses). As will be described in Section A.1.2, there is an upper limit to the shaft rotation rate and hence speed and resolution of the detected motion. When this limit is exceeded, the information provided by the mouse is meaningless. The pulley used for these experiments (shown in Figure A.3) was sufficient for all the acceleration profiles used.



(a) Mouse pulley and extended shaft



(b) Rear earth-fixed wire base



(c) Front earth-fixed wire base

Figure A.3: Mouse pulley and fixed-earth wire assembly. (a) The shaft of the x-axis was extended and a pulley was attached to it. To the left of the track, an earth-fixed wire was stretched and ran from the front of the track (a) to the rear of the track (b). This earth-fixed wire was looped through the mouse pulley. As the cart was moved forward, the wire caused the pulley to rotate, which in turn caused the slotted disk of the mouse to rotate and hence record the resulting motion.

	D7	D6	D5	D4	D3	D2	D1	D0
Byte 1	–	1	LB	RB	Y7	Y6	X7	X6
Byte 2	–	0	X5	X4	X3	X2	X1	X0
Byte 3	–	0	Y5	Y4	Y3	Y2	Y1	Y0

Table A.1: Microsoft serial mouse three byte data packet. LB and RB represent the state of the left and right buttons and are set to 1 when the corresponding mouse button is pressed. X7-X0 and Y7-Y0 are signed bytes and indicate the amount of movement in the X and Y directions respectively.

### Microsoft two-button serial mouse protocol

Communication between the serial mouse and the PC takes place at 1200bps (bits per second), using seven data bits and one stop bit. In addition, the DTR and RTS lines must be positive and the RTS-CTS lines should not be shorted. Information is sent from the mouse to the PC during every mouse event (e.g., every time the mouse state changes), which occurs when the mouse has moved or its buttons have been pressed. The information sent to the PC is a data packet consisting of three bytes which encode the amount moved in the X and Y axis and whether the left and right buttons were pressed. The format of the three byte data packet is listed in Table A.1. Referring to this table, LB and RB represent the state of the left and right buttons and are set to 1 when the corresponding mouse button is pressed. X7-X0 and Y7-Y0 are signed bytes and indicate the amount of movement in the X and Y directions respectively and the “–” denotes a value that may be either 0 or 1 and may therefore be ignored.

Movement in the X and Y axis is encoded using a signed byte thereby allowing for movement in both directions (e.g., positive and negative) for both axis. The maximum encoder counts for each mouse event is therefore restricted to  $\pm 127$  (e.g., 127 in either direction). The maximum update rate for the Microsoft serial mouse is 40 times each second, thereby restricting the maximum number of encoder counts each second to 5080 (e.g.,  $127 \times 40$ ) [12]. In addition, typical serial mice are capable of handling between 100 and 400 counts per inch (CPI) (or between 3937 and 15,748 counts per meter) therefore, a 100 CPI mouse can be moved, in either the X or Y axis, at a maximum speed of 50.8 inches each second (or 1.29 meters each second), while a 400 CPI mouse can be moved at a rate of 12.7 inches each second (or 0.32) meter each second) [12]. Attempting to move the mouse faster than its maximum allowable rate or over a larger distance (in one second) will cause the mouse to saturate thereby resulting in meaningless distance measurements.

As previously described, for the experiments which contained physical motion of the cart, the cart was either accelerated following one of five pre-defined acceleration profiles ( $0.012\text{m.s}^{-2}$ ,  $0.025\text{m.s}^{-2}$ ,  $0.05\text{m.s}^{-2}$ ,  $0.1\text{m.s}^{-2}$  and  $0.2\text{m.s}^{-2}$ ). As shown in Figure A.3, attached to the extended mouse shaft is a large pulley. However, initially, a much smaller pulley was used. Use of the smaller pulley resulted in 5400 encoder counts each meter and this resolution was sufficient for all but the  $0.1\text{m.s}^{-2}$  acceleration profile. While being moved

with this acceleration profile, the cart moved faster than the mouse could be updated causing the encoder to saturate (e.g., its output was meaningless). In order to reduce the encoder resolution and therefore increase the allowable distance travelled each second, the original smaller pulley was replaced with the larger pulley illustrated in Figure A.3.

### Serial mouse calibration

The output produced by the serial mouse is the encoder counts. During the motion of the cart, from the time the cart begins moving until the time the subject presses the button to indicate the target has been reached, the mouse encoder counts are accumulated. However, the desired experimental output for each trial is not distance specified in encoder counts but rather distance specified in meters. The number of encoder counts per meter (CPM)  $E_m$  was determined, by moving the cart (and therefore mouse and encoder assembly), along the entire length of the track (six meters), and recording the number of encoder counts at each marked one meter intervals along the track, and then averaging the results. Mathematically, this can be expressed as follows:

$$E_m = \frac{1}{N} \sum_{i=1}^N E_i \quad (\text{A.2})$$

where,  $N = 6$  and  $E_i$  is the total encoder counts in the one meter interval from  $i - 1$  meters to  $i$  meters. After performing this process, it was determined  $E_m = 1119.4$  CPM. It was also observed that the difference between the total encoder counts for each one meter interval was actually very small (e.g., under 10), verifying the accuracy and precision of distance recording using this simple and inexpensive mouse. Once  $E_m$  was calculated, the target distance  $d_t$  expressed in meters per second (e.g., the distance, from the starting position to the point the subject perceives the target to be at) is obtained as follows:

$$d_t = \frac{E_t}{E_m} \quad (\text{A.3})$$

where  $E_t$  is the total number of encoder counts accumulated beginning from the time the cart begins moving to the time the button is pressed by the subject and  $E_m = 1119.4$ .

<b>Specification</b>	<b>Value</b>
Processor	AMD-K6 3D Processor
Available RAM	128MB
Operating System	Microsoft Windows 98
Hard Disk Capacity	5GB
Audio Card	ESS Solo-1 PCI

Table A.2: Laptop PC specifications.

### A.1.3 Communicating with the serial mouse

The serial mouse was controlled with a Compaq Presario 1692 laptop PC (see Table A.2 for a list of the laptop's specifications). All software, including the software relative to the serial port, was written in Java (Java SDK 1.2.1). Communications with the serial port was performed with Sun Microsystem's Java Communications API 2.0. The API is very simple to use and certainly abstracts many of the details regarding serial communications from the user. The software was a GUI based program which recorded all necessary data per trial for each subject.

## Appendix B

# Motor assembly and controller

In this appendix greater information, including technical details, will be provided regarding the motor, motor controller and pulley assemblies used to move (pull) the motion carts following the specified acceleration or constant velocity profiles.

### B.1 Motor and motor controller

For the experiments which consisted of physical motion, the cart was pulled following a pre-defined motion profile generated with an EG & G MT-5330 servo motor (see Figure B.1(a)), mounted on a custom built platform, controlled by a Galil DMC-630 motion controller and power amplifier (see Figure B.1(b)). Briefly, a servo motor contains an output shaft which can be made to rotate to some specified angular position at some specified rate, by providing the servo an analog signal of some particular voltage. Provided the voltage of this analog signal is maintained (un-changed), the shaft will maintain this position [49]. The signal necessary to drive the motor is generated by the motion controller and power amplifier. The amplifier receives an analog signal (*coded signal*), typically in the range of  $\pm 10\text{V}$ , from the motor controller. In the *current mode* of operation (the mode of the power amplifier used in this work), a current, directly proportional to the input voltage, is generated by the amplifier and fed to the motor. By sending the appropriate coded analog signal, the shaft of the servo, via the motor controller and amplifier, will be rotated to some particular angular position, at some specific rate of acceleration or velocity. Typically, an *incremental encoder* is attached to the servo motor's shaft. The incremental encoder is an electrical device which generates  $N$  electrical pulses for each revolution of the shaft. By counting the number of pulses during some time interval, the speed and acceleration of the shaft can be determined. All motor

motions are thus specified in encoder counts.

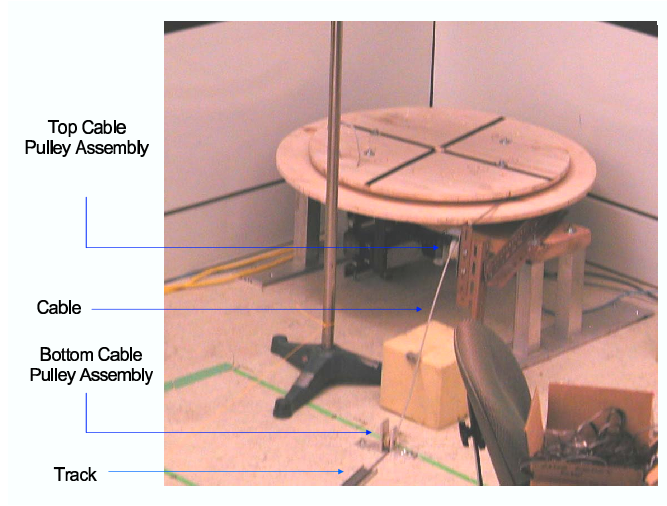
Steel cable connects the cart to the motor via several pulley assemblies (see Figure B.1(c)). It was observed that keeping the cable as close as possible to ground level minimizes the “slack” (flex) in the cable thereby decreasing the amount of “jerkiness” encountered throughout the motion profile but which is most pronounced during the start of the motion. The two cable pulley assemblies illustrated in Figure B.1(b) allowed the cable to be essentially on the ground. As the cart is pulled forward, the steel cable is collected (wound around) the “top pulley” illustrated in Figure B.1(b,d) As shown in Figure B.1(d), the top-pulley consists of three individual components, the top disk, middle disk and bottom disk. The radius of the middle disk determines the allowable range of accelerations. Decreasing the radius will shift the range of accelerations downwards (e.g., smaller minimum acceleration but smaller maximum acceleration), while increasing the radius causes the range of accelerations to shift upwards (e.g., increase in the minimum acceleration and increase in the maximum acceleration). In this study, the accelerations ranged from  $0.012\text{m}\cdot\text{s}^{-2}$  (low acceleration) to  $0.2\text{m}\cdot\text{s}^{-2}$  (high acceleration) and several middle disk sizes were initially tested to allow for motions in this range. It clearly became evident that as the radius of the middle disk is decreased, the stability of the higher acceleration profiles quickly degrades. In particular, the motion of the higher acceleration appears to be much faster than actually specified leading to a potentially dangerous situation, when, for example, the radius of the middle disk is less than 0.10m. Although in this study an acceleration below  $0.012\text{m}\cdot\text{s}^{-2}$  was desirable, a compromise between allowable acceleration ranges and safety was reached using a radius of 0.18m, leading to the range of accelerations from  $0.012\text{m}\cdot\text{s}^{-2}$  to  $0.2\text{m}\cdot\text{s}^{-2}$ .

## B.2 Track

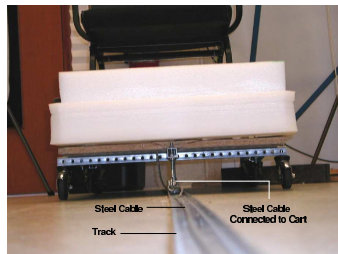
To ensure the cart followed a straight trajectory throughout its entire motion profile and did not veer from side-to-side, thereby ensuring a “smooth” acceleration profile, the cart was forced to follow a track placed on the floor. As shown in Figure B.2, the track itself consists of two 3.6m meter pieces of aluminum. Both pieces were combined to provide a total track length of 7.2m. Given the length of cart itself was just over one meter, this allowed for a track length of approximately six meters. Since the cart is accelerated throughout the motion trials, the last two meters are used to decelerate the cart to a complete stop. Therefore, the total usable track length is essentially four meters (e.g., maximum target distances are restricted to four meters). As shown in Figure B.2, a “peg” was attached (centered) underneath both the front and rear end of the cart. The diameter of both pegs (0.031m each) was just slightly smaller than the width of the track (0.038m), forcing the pegs to remain within the track throughout the entire motion profile. The diameter of the pegs was small enough so that it did not obstruct movement within the track yet large enough to ensure there was little room to move within the track. Since there was little room for the peg to move within the track, the pegs ensured the cart followed the track and therefore a “straight line” path for the entire



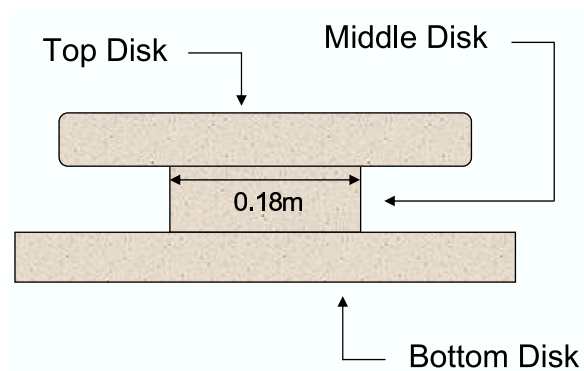
(a) EG & G MT-5330 servo motor and gears.



(b) Pulley assemblies.



(c) Steel cable connected to front of cart.



(d) Top pulley construction

Figure B.1: Servo motor and pulley assemblies. (a) Servo motor and gears. (b) Pulley assemblies, including the top pulley which collects the steel cable and the two “cable pulleys” used to feed the cable to the top pulley. (c) The steel cable used to pull the cart is connected to the front of the cart. (d) Construction of the top pulley. The top pulley consists of three disks: the upper disk, middle disk and lower disk. The size of the middle disk determines the allowable range of accelerations.



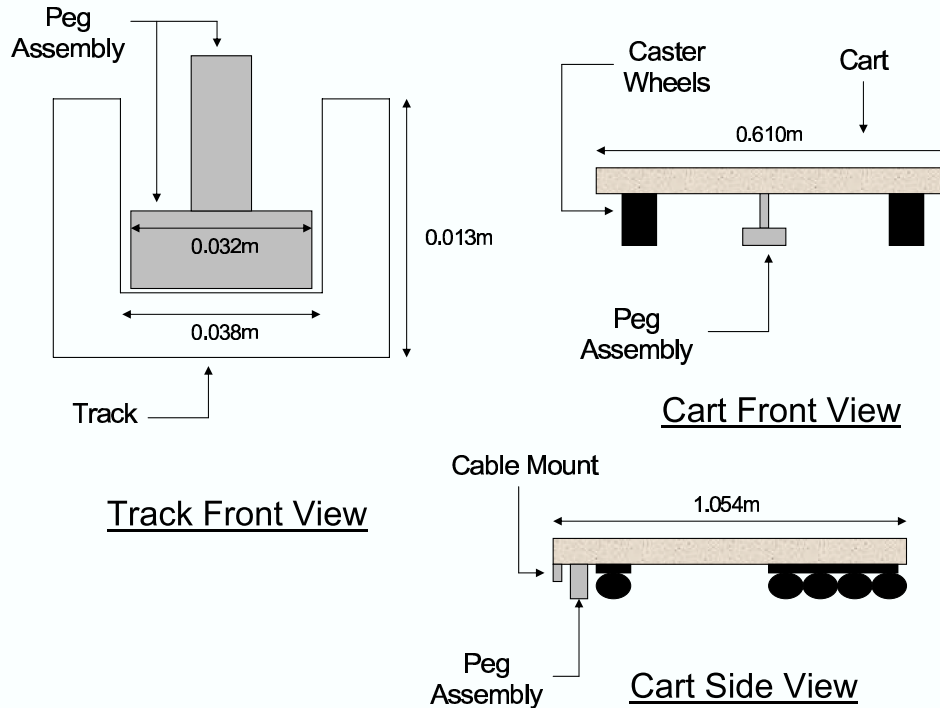


Figure B.2: Track and cart peg assemblies.

motion trajectory.

### B.3 Controlling the motor

As previously described, the motor is controlled with a Galil DMC-630 multi-axis motion controller via a “host” computer. Through the host computer and a simple programming language, the motor can be programmed to “move” following various motion profiles, including constant acceleration and constant velocity profiles required for this work. The controller programming language consists of an assembly-like instruction set with two-letter uppercase “English-like” commands. For example, the command “TP X” will output the position (in encoder counts) of the X-axis, while the command “SP N” will set the speed (velocity) of the motor to “N” encoder counts per second. Although the controller is capable of handling complex motion profiles over multiple axis, for this work, all motion profiles were linear (e.g., following a straight line path) and restricted to a single axis. In order to accomplish the motion profiles required for these experiments, a modified trapezoidal motion profile is used. As shown in Figure B.3, a (non-modified) trapezoidal profile consists of a period of acceleration, followed by a period of constant velocity and finally a period of deceleration before coming

to a complete stop. The trapezoidal motion profile can be programmed using a very small set of instructions. Essentially, the rate of acceleration, constant velocity and deceleration are specified in encoder counts. In other words, velocity and acceleration are specified in encoder counts per second  $enc_{count}S^{-1}$  and encoder counts per seconds squared  $enc_{count}S^{-2}$  respectively.

In this work, distance traveled is of interest and being measured hence a method of calibration is required in order to convert encoder counts to distance and vice versa. In other words, the number of encoder counts per meter  $M_e$  is required to convert encoder counts to distance measured in meters. In order to determine this value, after resetting the motion controller (e.g., so the motor position determined with a “TP” command is 0), the motion cart was pulled for one meter and then the position of the motor (in encoder counts) was obtained (using the “TP” command). After repeating this process several times and averaging the results, it was determined that:

$$M_e = 75861.80 \tag{B.1}$$

As mentioned,  $E_m$  specifies the number of encoder counts each meter. With this value known, the controller motion profile values (acceleration  $AC$ , constant velocity  $SP$  and deceleration  $DC$ ), required by the controller to perform the trapezoidal motion profile can be easily specified as follows (see Section B.3.1 for complete listing of the controller source code):

$$PR = E_m \times d_t \tag{B.2}$$

$$AC = a \times M_e \times d_a \tag{B.3}$$

$$SP = v \times M_e \times d_v \tag{B.4}$$

$$DC = d \times M_e \times d_d \tag{B.5}$$

where  $a$  is the desired rate of acceleration,  $v$  is the desired velocity,  $d$  is the desired rate of deceleration and  $d_t = 6m$ ,  $d_a = 4m$ ,  $d_v = 0m$  and  $d_d = 2m$  are the total distance the cart will move, accelerate, move at constant velocity and decelerate respectively. Although the target distance varied between one of four distances (e.g., 1m - 4m), the value of  $d_a$  was fixed to the maximum target distance of 4m to account for any over-estimation of the target distance by any of the subjects (e.g., moving past the original target distance). Of course, this may lead to problems if a 4m target was over-estimated, however, as discussed in Chapter 4, over-estimation of the target rarely occurred and did not occur for any of the 4m targets distances.

For the constant acceleration profiles used in experiments one, three and four, there was

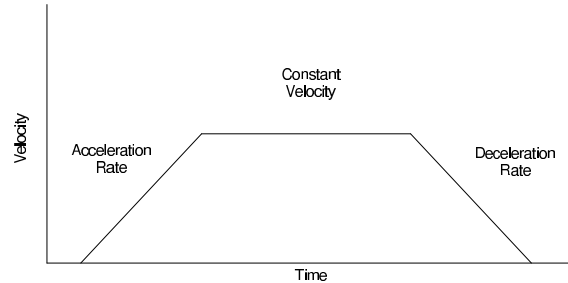


Figure B.3: Trapezoidal velocity motion profile. Period of acceleration followed by a period of constant velocity and deceleration.

no period of constant velocity but rather, the motion profile consisted of a period of constant acceleration immediately followed by a period of constant deceleration (e.g., a triangular profile). In order to achieve constant acceleration immediately followed by a period of deceleration and hence no constant velocity,  $SP$  was set to an arbitrary large value which would never be reached given the rate of acceleration over the maximum of four meters. As a result, the cart continued to accelerate for four meters and then immediately following this, it started decelerating for two meters until it came to a complete stop exactly six meters from the starting position.

The trapezoidal motion profile is (in theory) very simple to perform and to specify, however, in practise, the actual motion profiles experienced by the cart is certainly not as expected, and depending on the acceleration, at times not a constant acceleration at all but rather appeared to be a constant velocity. The motion profile can be measured by having the cart move through some specified profile (pulled by the motor) while recording the total distance traveled at regular time intervals, from the start of the motion to its end, using the equipment and techniques described in Appendix A. By examining the resulting profiles for each of the desired acceleration profiles, it was clearly evident they were not as required. In fact, several of the profiles produced a constant velocity type profile which could easily be determined visually, by looking at the cart while it underwent its motion. For others which did accelerate, it was determined that the rate of acceleration was not the rate specified but rather, varied significantly.

As described in [21], during the execution of a motion profile by the motor controller, the controller will continuously determine the position of the motor (via the incremental encoder) and compare the motor's actual position with the desired position. The difference between the desired and actual positions is known as the positional error and the controller will attempt

to minimize this error with a stabilizing filter. The stabilizing filter of the controller used in this work is known as a proportional-integral-derivative (PID) filter specified by the three terms proportional (KP), integral (KI) and derivative (KD). Therefore, depending on the value of these parameters, the actual motion profile may not necessarily be the same as the specified motion profile. Furthermore, there is no method or technique for determining the appropriate values but rather, according to the controller distributor (Electromate Industrial Sales Ltd), determining these values is a “trial and error process” [28]. In addition, incorrect PID parameters can lead to an under-damped, over-damped or an unstable system [28]. After experimenting with many different values for these parameters and adjusting the values of *AC*, *SP* and *DC* slightly, the desired acceleration profiles were obtained. A graphical illustration of the resulting profiles, measured using the techniques described in Appendix A, is provided in Figure 3.4 of Chapter 3. Finally, there are several other parameters which may be specified and affect the desired motion profile. For example, the power amplifier used to generate the appropriate current to operate the servo motor as desired, includes a *current gain* parameter which specifies the amount to amplify each 1V of the coded signal it receives [49]. Changes to this parameter can also affect the desired motion profile and may once again require further “trial and error” experimenting before an optimal setting is determined. Further details regarding these parameters can be found in [21, 28, 49].

### B.3.1 Controller programs: source code

In this section, the controller source code for each of the motion profiles used in this study is provided. A separate program was written for each of the desired profiles, however, the program structure is essentially identical except the acceleration, deceleration and constant velocity values differ. The controller interface allows for commands to be issued directly from the host computer (*immediate mode*) or, alternatively, multiple commands can be combined into a stored program (*program mode*). In program mode, the beginning of the program begins with the line “# NAME” (where NAME indicates the name of the program) and ends with the line “EN”. This allows a stored program too contain many sub-programs. To execute any one particular sub-program, the command “XQ#NAME” is issued, where, once again, ‘NAME’ is the name of the program to be executed. Prior to listing the code, several of the instructions which were not previously described but are used in the programs will be defined.

**NO** A comment for the programmer’s use only. Ignored by the controller.

**MG** ‘MESSAGE’ Display the message ‘MESSAGE’ to the screen of the host computer.

**PR N** Relative distance (in encoder counts). The motor will move (rotate) ‘X’ encoder counts during the entire motion profile.

**GN N** Set the gain of the power amplifier to ‘X’.

**DP N** Define (set) the position of the X axis to N

## BG X Begin motion of axis 'X'

The following code listing is for the slowest acceleration profile, 0.012m/s/s. As mentioned, the 'PR' command specifies the total distance (in encoder counts) for the motor to move. As shown in the code listing below, 'PR' is set to a negative value. The negative value simply changes the direction of movement and ensures the cart is moved towards the motor itself as opposed to having the cart move away from the motor (if the value was positive).

```
#A
NO 75861.80 IS 1 METER
MG CONSTANT ACC 0.012m$/s$/s
GN 3
DP 0
PR -75861.80 * 6
AC 75861.80 * 0.02875
DC 75861.80 * 0.0575
SP 75861.80 * 0.45
BGX
EN
```

The following code listing is for the 0.025m/s/s acceleration profile.

```
#B
NO 75861.80 IS 1 METER
MG CONSTANT ACC 0.025m$.$s$^-2$
GN 3
DP 0
PR -75861.80 * 6
AC 75861.80 * 0.02875
DC 75861.80 * 0.0575
SP 75861.80 * 0.45
BGX
EN
```

The following code listing is for the 0.05m/s/s acceleration profile.

```
#C
NO 75861.80 IS 1 METER
MG CONSTANT ACC 0.05m$.$s$^-2$
GN 3
DP 0
PR -75861.80 * 6
AC 75861.80 * 0.0575
DC 75861.80 * 0.23
SP 75861.80 * 0.63
BGX
EN
```

The following code listing is for the 0.1m/s/s acceleration profile.

```
#D
NO 75861.80 IS 1 METER
MG CONSTANT ACC 0.1m$.s$^-2$
GN 3
DP 0
PR -75861.80 * 6
AC 75861.80 * 0.115
DC 75861.80 * 0.23
SP 75861.80 * 0.89
BGX
EN
```

Finally, the following code listing is for the fastest acceleration profile of 0.2m/s/s.

```
#E
MG CONSTANT ACC 0.2m$.s$^-2$
NO 75861.80 IS 1 METER
GN 3
DP 0
PR -75861.80 * 6
AC 75861.80 * 0.23
DC 75861.80 * 0.46
SP 75861.80 * 1.26
BGX
EN
```

# Bibliography

- [1] J. A. Altman and O. V. Viskov. Discrimination of perceived movement velocity used for fused auditory image in dichotic stimulation. *Journal of the Acoustical Society of America*, 61:816–819, 1977.
- [2] D. H. Ashmead, D. L. Davis, and A. Northington. Contribution of listeners’ approaching motion to auditory distance perception. *Journal of Experimental Psychology: Human Perception and Performance*, 21:239–256, 1995.
- [3] F. Baumgart, B. Gaschler-Markefski, M. G. Woldorff, M. G. Heinze, and H. Scheich. A movement-sensitive area in auditory cortex. *Nature*, 400:724–726, 1996.
- [4] R. Begault. *3-D Sound for Virtual Reality and Multimedia*. Academic Press Professional, Cambridge, MA. USA, 1994.
- [5] A. J. Benson and J. R. Scott. Thresholds for the detection of the direction. *Aviation, Space, and Environmental Medicine*, 11:1088–1096, 1986.
- [6] M. Brain. <http://computer.howstuffworks.com/mouse2.htm>.
- [7] D. S. Brungart and W. M. Rabinowitz. Auditory localization of nearby sources. head related transfer functions. *Journal of the Acoustical Society of America*, 106(3):1465–1479, 1999.
- [8] Gianna C, S. Heimbrand, and M. Gresty. Thresholds for dection of motion direction during passive lateral whole-body acceleration in normal subjects and patients with bilateral loss of labyrinthe function. *Brain Research Bulletin*, 40:435–439, 1996.
- [9] S. Carlile. *Virtual Auditory Space: Generation and Application*. R. G. Landes Company, Austin, TX. USA, 1996.
- [10] S. Carlile and V. Best. Discrimination of sound source velocity in human listeners. *Journal of the Acoustical Society of America*, 111(2):1026–1035, 2002.
- [11] P. D. Coleman. An analysis of cues to auditory depth perception in free space. *Psychological Bulletin*, 60:302–315, 1963.
- [12] T. Engdahl. PC mouse information. <http://www.epanorama.net/documents/pc/mouse.html>.
- [13] M. A. Ericson. The relative salience of auditory motion cues. In *Proceedings of the 2001 IEEE Workshop on Applications of Signal Processing to Audio and Acoustics*, Mohonk Mountain House, New Paltz, NY. USA, 2001.
- [14] H. Fletcher and W. A. Munson. Loudness, its definition, measurement and calculation. *Journal of the Acoustical Society of America*, 5:82–108, 1933.

- [15] J. Garas. *Adaptive 3D Sound Systems*. Kluwer Academic Publishers, Norwell, MA. USA, 2000.
- [16] D. W. Grantham. Detection and discrimination of simulated motion of auditory targets in the horizontal plane. *Journal of the Acoustical Society of America*, 79:1039–1049, 1986.
- [17] D. W. Grantham. Auditory motion perception: Snapshots revisited. In R. H. Gilkey and T. R. Anderson, editors, *Binaural and spatial hearing in real and virtual environments*, pages 295–313. Lawrence Erlbaum Associates, Hillsdale, NJ USA, 1997.
- [18] R. Guski. Acoustic tau: An easy analog to visual tau? *Ecological Psychology*, 4:189–197, 1992.
- [19] L. R. Harris, M. Jenkin, and D. C. Zikovitz. Visual and non-visual cues in the perception of linear self motion. *Experimental Brain Research*, 135:12–21, 2000.
- [20] I. P. Howard and B. J. Rogers. *Seeing in Depth*, volume 2. University of Toronto Press, Ontario, Canada, 2002.
- [21] Galil Motion Control Inc. System elements. Technical refernce, Galil Motion Controls Inc., Rocklin, CA. USA.
- [22] I. Israel, N. Chaptuis, S. Glasauer, O. Charade, and A. Berthoz. Estimation of passive horizontal linear whole-body displacement in humans. *Journal of Neurophysiology*, pages 1270–73, 1993.
- [23] R. L. Jenison. On acoustic information for motion. *Ecological Psychology*, 9(2):131–151, 1997.
- [24] R. L. Jenison and R. A. Lutfi. Kinematic synthesis of auditory motion. *Journal of the Acoustical Society of America*, 92, 1992.
- [25] D. N. Lee. A theory of visual control of braking based on information about time to collision. *Perception*, 5:437–459, 1976.
- [26] D. N. Lee. Visuo-motor coordination in space-time. In G. E. Stelmach and J. Requin, editors, *Tutorials on Motor Behavior*, pages 281–295. North Holland Publishers, New York, NY. USA., 1980.
- [27] D. N. Lee, F. R. van der Weel, T. Hitchcock, E. Matejowsky, and J. D. Pettugrew. Common principle on guidance by echolocation and vision. *Journal of Comparative Physiology*, A 171:563–571, 1992.
- [28] Electromate Industrial Sales Ltd. Introductory guide to programming galil motion controllers. Version 2.0.
- [29] R. A. Lutfi and W. Wang. Correlated analysis of acoustic cues for the discrimination of auditory motion. *Journal of the Acoustical Society of America*, 106(2):919–928, 1999.
- [30] V. V. Marlinsky. Vestibular and vestibulo-proprioceptive perception of motion in the horizontal plane in blind-folded man. I estimations of linear displacement. *The Journal of Neuroscience*, pages 389–394, 1999.
- [31] B. C. J. Moore. *An Introduction to the Psychology of Hearing*. Academic Press Limited, San Diego, CA. USA, 1989.
- [32] B. C. J. Moore, B. R. Glassberg, and Thomas Baer. A model for the prediction of thresholds, loudness and partial loudness. *Journal of the Audio Engineering Society*, 45(4):224–239, 1997.
- [33] M. Naguib and H. Wiley. Estimating the distance to a sound: Mechanisms and adaptations for long-range communications. *Animal Behavior*, 62:825–837, 2001.



- [34] J. G. Neuhoff. An adaptive bias in the perception of looming auditory motion. *Ecological Psychology*, 13(2):87–110, 2001.
- [35] J. G. Neuhoff. Auditory motion and localization. In J. G. Neuhoff, editor, *Ecological Psychoacoustics*, chapter four, pages 87–111. Elsevier Academic Press, San Diego, CA. USA, 2004.
- [36] S. H. Nielson. Auditory distance perception in different rooms. *Journal of the Audio Engineering Society*, 41(10):755–770, 1993.
- [37] D. R. Perrot, B. Costantino, and J. Ball. Discrimination of moving events which accelerate or decelerate over the listening interval. *Journal of the Acoustical Society of America*, 93:1053–1057, 1993.
- [38] J. P. Rauschecker and L. R. Harris. Auditory and visual neurons in the cat’s superior colliculus selective for the direction of apparent motion stimuli. *Brain Research*, 490:56–63, 1989.
- [39] D. W. Robinson and R. S. Dadson. A re-determination of the equal-loudness relations for pure tones. *British Journal of Applied Physics*, 7:166–181, 1956.
- [40] L. D. Rosenblum, C. Carello, and R. E. Pastore. Relative effectiveness of three stimulus variables for locating a moving sound source. *Perception*, 16:175–186, 1987.
- [41] L. D. Rosenblum, M. S. Gordon, and L. Jarquin. Echolocation by moving and stationary listeners. *Ecological Psychology*, 12(3):181–206, 2000.
- [42] L. D. Rosenblum, A. P. Wuestfeld, and H. M. Saldana. Auditory looming perception: Influences on anticipatory judgements. *Perception*, 22:1467–1482, 1993.
- [43] K. Saberi and E. R. Hafter. Experiments on auditory motion discrimination. In *Binaural and Spatial Hearing in Real and Virtual Environments*, chapter 16, pages 375–327. Laurence Erlbaum Associates Inc., Mahwah, NJ. USA, 1997.
- [44] W. Schiff and R. Oldak. Accuracy of judging time to arrival: Effects of modality, trajectory and gender. *Journal of Experimental Psychology Human Perception and Performance*, 16:303–316, 1990.
- [45] B. K. Shaw, R. S. McGowan, and M. T. Turvey. An acoustic variable specifying time-to-contact. *Ecological Psychology*, 3(3):253–261, 1991.
- [46] B. G. Shin-Cunningham. Distance cues for virtual auditory space. In *Proceedings of the First IEEE Pacific-Rim Conference on Multimedia.*, Sydney, Australia, December 2000.
- [47] B. E. Stein and M. A. Meredith. *The Merging of the Senses*. MIT Press, Cambridge, MA. USA, 1993.
- [48] T. A. Stoffregen and J. B. Pittenger. Human echolocation as a basic form of perception and action. *Ecological Psychology*, 7(3):181–216, 1995.
- [49] J. Tal. *Step-by-Step Design of Motion Control Systems*. Galil Motion Control Inc., Sunnyvale, CA. USA, 1994.
- [50] J. R. Tresilian. Perceptual information for the timing of interceptive action. *Perception*, 19:223–239, 1990.
- [51] von Bekesy. *Experiments in Hearing*. McGraw Hill, New York, NY. USA, 1960.

- [52] W. Wang and R. A. Lutfi. Thresholds for detection of a change in the displacement, velocity and acceleration of a synthesized sound-emitting source. *Journal of the Acoustical Society of America*, 95(5):2897, 1994.
- [53] W. Waugh, T. Z. Strybel, and D. R. Perrott. Perception of moving sounds: velocity discrimination. *Journal of Auditory Research*, 19:103–110, 1979.
- [54] F. L. Wightman and D. J. Kistler. Sound localization. In W. Yost, A. Popper, and R. Fay, editors, *Springer Handbook of Auditory Research: Human Psychophysics*, volume 3, pages 155–192. Springer-Verlag Inc., New York NY. USA, 1993.
- [55] R. Wolfson and J. M. Pasachoff. *Physics with Modern Physics*. HarperCollins College Publishers, New York, NY. USA, 1995.
- [56] S. M. Wuerger, M. Hofbauer, and G. Meyer. The integration of auditory and visual motion signals at threshold. *Perception and Psychophysics*, 65(8):1188–1196, 2003.
- [57] P. Zahorik. Auditory distance perception: A literature review. Phd Preliminary Examination, University of West Maddison, Department of Psychology, August 1996.